

Doubly heavy tetraquarks in an extended chromomagnetic model

Xin-Zhen Weng,^{1,2,*} Wei-Zhen Deng,^{3,†} and Shi-Lin Zhu^{1,3,4,‡}

¹Center of High Energy Physics, Peking University, Beijing 100871, China

²School of Physics and Astronomy, Tel Aviv University, Tel Aviv 69978, Israel

³School of Physics and State Key Laboratory of Nuclear Physics and Technology, Peking University, Beijing 100871, China

⁴Collaborative Innovation Center of Quantum Matter, Beijing 100871, China

(Dated: October 6, 2021)

Using an extended chromomagnetic model, we perform a systematic study of the masses of the doubly heavy tetraquarks. We find that the ground states of the doubly heavy tetraquarks are dominated by color-triplet $|(qq)^3c(\bar{Q}\bar{Q})^3c\rangle$ configuration, which is opposite to that of the fully heavy tetraquarks. The combined results suggest that the color-triplet configuration becomes more important when the mass difference between the quarks and antiquarks increases. We find three stable states which lie below the thresholds of two pseudoscalar mesons. They are the $IJ^P = 01^+ nn\bar{b}$ tetraquark, the $IJ^P = 00^+ nn\bar{c}$ tetraquark and the $J^P = 1^+ ns\bar{b}$ tetraquark.

I. INTRODUCTION

Besides the conventional meson and baryon composed of quark-antiquark pair and three quarks, there also exist hadrons composed of more than three quarks, or gluons. These states are called exotic states, such as the tetraquark [1, 2], pentaquark [3, 4], molecule [5–7], glueball [8, 9], hybrid [10, 11], etc. In 2003, the first charmoniumlike state $X(3872)$ was observed by the Belle Collaboration in the exclusive $B^\pm \rightarrow K^\pm \pi^+ \pi^- J/\psi$ decays [12]. Its quantum number is $I^G J^{PC} = 0^+ 1^{++}$ [13]. The discovery of $X(3872)$ opens a new era of the hadron spectroscopy. Lots of charmoniumlike and bottomoniumlike states were found since then, such as the $Y(4260)$ [14], $Z_c(3900)$ [15, 16], $Z_b(10610)$ and $Z_b(10650)$ [17] states. In the fully heavy sector, the LHCb collaboration observed a narrow structure and a wide structure in the J/ψ -pair invariant mass spectrum in the range of $6.2 \sim 7.2$ GeV, which could be all-charm hadrons [18]. More details can be found in Refs. [19–26] and references therein.

The heavy quarks in these states are all in hidden flavor(s). In 2017, the LHCb Collaboration observed the Ξ_{cc}^{++} in the $\Lambda_c^+ K^- \pi^+ \pi^+$ decay channel [27]. Its mass was determined to be $3621.40 \pm 0.72(\text{stat.}) \pm 0.27(\text{syst.}) \pm 0.14(\Lambda_c^+)$ MeV. This is the first doubly heavy baryon observed in experiment. The Ξ_{cc}^{++} baryon gives implications for the doubly heavy tetraquarks [28, 29], which are exotic states with open heavy flavors. Recently, the LHCb Collaboration observed a very narrow state in the $D^0 D^0 \pi^+$ mass spectrum [30–33]. Under the $J^P = 1^+$ assumption, its mass with respect to the $D^{*+} D^0$ and width are

$$\delta m_{\text{BW}} = -273 \pm 61 \pm 5_{-14}^{+11} \text{ keV}, \quad (1)$$

and

$$\Gamma_{\text{BW}} = 410 \pm 165 \pm 43_{-38}^{+18} \text{ keV}, \quad (2)$$

respectively. The statistic significance for the signal is over 10σ , while that for $\delta m_{\text{BW}} < 0$ is 4.3σ . This structure is consistent with the DD^* molecule interpretation predicted by Li *et al.* within the one-boson-exchange (OBE) model [34]. The discovery of the T_{cc}^+ inspired many related studies [35–44]. Actually, the doubly heavy tetraquarks have been studied extensively in the literature, with models like the quark model [1, 45–72], QCD sum rules [73–83], Lattice QCD [84–102], the OBE potentials [34, 103–107], chiral perturbation theory [108–111], etc. Their production has also been studied (for instance, see Refs. [112, 113]). The studies suggest that the masses of some of the doubly heavy tetraquarks are lighter than the thresholds of two mesons, which makes them stable against the strong and electromagnetic decays. For example, Du *et al.* [76] studied the $QQ\bar{q}\bar{q}'$ ($Q = c, b$ and $q, q' = u, d, s$) in the QCD sum rules. They found that the $bb\bar{q}\bar{q}'$'s are stable. The stableness of doubly heavy tetraquarks is also supported by the lattice QCD calculations. Leskovec *et al.* [100] used lattice QCD to investigate the spectrum of the $\bar{b}bud$ four-quark system with quantum numbers $I(J^P) = 0(1^+)$, and obtained a binding energy of $(-128 \pm 24 \pm 10)$ MeV, corresponding to the mass $10476 \pm 24 \pm 10$ MeV. Mohanta and Basak [102] studied the $bb\bar{u}\bar{d}$ states on lattice using non relativistic QCD (NRQCD) action for bottom and highly improved staggered quark (HISQ) action for the light up/down quarks. They got the binding energy for the $1^+ bb\bar{u}\bar{d}$ tetraquark system to be $-189(18)$ MeV compared to the BB^* . Using Ξ_{cc}^{++} mass as input, Karliner and Rosner [29] predicted that the mass of the ground state of $IJ^P = 01^+$ doubly charm tetraquark (T_{cc}) to be 3882.2 ± 12 MeV in the chromomagnetic model.

In the quark model [114–118], the mass of hadron can be decomposed into the quark masses, the kinetic energy and the potentials which include the color-independent Coulomb and confinement interactions, and the hyperfine interactions like the spin-spin, spin-orbit, and tensor terms. If we restrict to the S -wave states, the spin-orbit and tensor interactions do not contribute. We can use the extended chromomagnetic model [1, 58, 118–127]. In this model, the masses of S -wave hadrons consist of effective

* xzhweng@pku.edu.cn

† dwz@pku.edu.cn

‡ zhysl@pku.edu.cn

quark masses, the color interaction and the chromomagnetic interaction. This simplified model gives good account of all S -wave mesons and baryons [125]. In this work, we use the extended chromomagnetic model to study the S -wave doubly heavy tetraquarks. With the wave function obtained, we further use a simple method to estimate the partial decay ratios of the tetraquark states. In Sec. II we introduce the methods of present work, The numerical results are presented and discussed in Sec. III. We conclude in Sec. IV.

II. FORMALISM

A. Hamiltonian

In the chromomagnetic model, the Hamiltonian of the S -wave hadron reads [123, 125–131]

$$H = \sum_i m_i + H_{\text{CE}} + H_{\text{CM}} \quad (3)$$

where m_i is the effective mass of i th quark, H_{CE} is the chromoelectric (CE) interaction [123, 125–127]

$$H_{\text{CE}} = - \sum_{i < j} a_{ij} \mathbf{F}_i \cdot \mathbf{F}_j, \quad (4)$$

and H_{CM} is the chromomagnetic (CM) interaction [1, 26, 120–122]

$$H_{\text{CM}} = - \sum_{i < j} v_{ij} \mathbf{S}_i \cdot \mathbf{S}_j \mathbf{F}_i \cdot \mathbf{F}_j. \quad (5)$$

Here, a_{ij} and $v_{ij} \propto \langle \alpha_s(r_{ij}) \delta(\mathbf{r}_{ij}) \rangle / m_i m_j$ are effective coupling constants which depend on the constituent quark masses and the spatial wave function. $\mathbf{S}_i = \boldsymbol{\sigma}_i / 2$ and $\mathbf{F}_i = \boldsymbol{\lambda}_i / 2$ are the quark spin and color operators. For the antiquark,

$$\mathbf{S}_{\bar{q}} = -\mathbf{S}_q^*, \quad \mathbf{F}_{\bar{q}} = -\mathbf{F}_q^*. \quad (6)$$

Since

$$\begin{aligned} & \sum_{i < j} (m_i + m_j) \mathbf{F}_i \cdot \mathbf{F}_j \\ &= \left(\sum_i m_i \mathbf{F}_i \right) \cdot \left(\sum_i \mathbf{F}_i \right) - \frac{4}{3} \sum_i m_i, \end{aligned} \quad (7)$$

and the total color operator $\sum_i \mathbf{F}_i$ nullifies any color-singlet physical state, we can rewrite the Hamiltonian as [125–127]

$$H = -\frac{3}{4} \sum_{i < j} m_{ij} V_{ij}^{\text{C}} - \sum_{i < j} v_{ij} V_{ij}^{\text{CM}}, \quad (8)$$

where

$$m_{ij} = (m_i + m_j) + \frac{4}{3} a_{ij}, \quad (9)$$

is the quark pair mass parameter. $V_{ij}^{\text{C}} = \mathbf{F}_i \cdot \mathbf{F}_j$ and $V_{ij}^{\text{CM}} = \mathbf{S}_i \cdot \mathbf{S}_j \mathbf{F}_i \cdot \mathbf{F}_j$ are the color and CM interactions between quarks.

B. Wave function

To investigate the masses of the tetraquarks, we need to construct the wave functions. The total wave function is a direct product of the orbital, color, spin and flavor wave functions. Here, the orbital wave function is symmetric since we only consider the S -wave states. Since the Hamiltonian does not contain a flavor operator explicitly, we first construct the color-spin wave function, and then incorporate the flavor wave function to account for the Pauli principle.

The spins of the tetraquarks can be 0, 1 and 2. In the $qq\bar{q}\bar{q}$ configuration, the possible color-spin wave functions $\{\alpha_i^J\}$ are listed as follows,

1. $J^P = 0^+$:

$$\begin{aligned} \alpha_1^0 &= |(q_1 q_2)_1^6 (\bar{q}_3 \bar{q}_4)_1^{\bar{6}}\rangle_0, \\ \alpha_2^0 &= |(q_1 q_2)_0^6 (\bar{q}_3 \bar{q}_4)_0^{\bar{6}}\rangle_0, \\ \alpha_3^0 &= |(q_1 q_2)_1^{\bar{3}} (\bar{q}_3 \bar{q}_4)_1^3\rangle_0, \\ \alpha_4^0 &= |(q_1 q_2)_0^{\bar{3}} (\bar{q}_3 \bar{q}_4)_0^3\rangle_0, \end{aligned} \quad (10)$$

2. $J^P = 1^+$:

$$\begin{aligned} \alpha_1^1 &= |(q_1 q_2)_1^6 (\bar{q}_3 \bar{q}_4)_1^{\bar{6}}\rangle_1, \\ \alpha_2^1 &= |(q_1 q_2)_1^6 (\bar{q}_3 \bar{q}_4)_0^{\bar{6}}\rangle_1, \\ \alpha_3^1 &= |(q_1 q_2)_0^6 (\bar{q}_3 \bar{q}_4)_1^{\bar{6}}\rangle_1, \\ \alpha_4^1 &= |(q_1 q_2)_1^{\bar{3}} (\bar{q}_3 \bar{q}_4)_1^3\rangle_1, \\ \alpha_5^1 &= |(q_1 q_2)_1^{\bar{3}} (\bar{q}_3 \bar{q}_4)_0^3\rangle_1, \\ \alpha_6^1 &= |(q_1 q_2)_0^{\bar{3}} (\bar{q}_3 \bar{q}_4)_1^3\rangle_1, \end{aligned} \quad (11)$$

3. $J^P = 2^+$:

$$\begin{aligned} \alpha_1^2 &= |(q_1 q_2)_1^6 (\bar{q}_3 \bar{q}_4)_1^{\bar{6}}\rangle_2, \\ \alpha_2^2 &= |(q_1 q_2)_1^{\bar{3}} (\bar{q}_3 \bar{q}_4)_1^3\rangle_2, \end{aligned} \quad (12)$$

where the superscript 3, $\bar{3}$, 6 or $\bar{6}$ denotes the color, and the subscript 0, 1 or 2 denotes the spin.

Next we consider the flavor wave function. There are six types of total wave functions when we consider the Pauli principle:

1. Type A: $\varphi_{\text{A}} = \{(n\bar{n}\bar{Q}\bar{Q})^{I=1}, s\bar{s}\bar{Q}\bar{Q}\}$

(a) $J^P = 0^+$:

$$\begin{aligned} \Psi_{\text{A}1}^{0+} &= \varphi_{\text{A}} \otimes \alpha_2^0, \\ \Psi_{\text{A}2}^{0+} &= \varphi_{\text{A}} \otimes \alpha_3^0, \end{aligned} \quad (13)$$

(b) $J^P = 1^+$:

$$\Psi_{\text{A}}^{1+} = \varphi_{\text{A}} \otimes \alpha_4^1, \quad (14)$$

(c) $J^P = 2^+$:

$$\Psi_A^{2^+} = \varphi_A \otimes \alpha_2^2, \quad (15)$$

2. Type B: $\varphi_B = \{(nn\bar{Q}\bar{Q})^{I=0}\}$ (a) $J^P = 1^+$:

$$\begin{aligned} \Psi_{B1}^{1^+} &= \varphi_B \otimes \alpha_2^1, \\ \Psi_{B2}^{1^+} &= \varphi_B \otimes \alpha_6^1, \end{aligned} \quad (16)$$

3. Type C: $\varphi_C = \{(nn\bar{c}\bar{b})^{I=1}, ss\bar{c}\bar{b}\}$ (a) $J^P = 0^+$:

$$\begin{aligned} \Psi_{C1}^{0^+} &= \varphi_C \otimes \alpha_2^0, \\ \Psi_{C2}^{0^+} &= \varphi_C \otimes \alpha_3^0, \end{aligned} \quad (17)$$

(b) $J^P = 1^+$:

$$\begin{aligned} \Psi_{C1}^{1^+} &= \varphi_C \otimes \alpha_3^1, \\ \Psi_{C2}^{1^+} &= \varphi_C \otimes \alpha_4^1, \\ \Psi_{C3}^{1^+} &= \varphi_C \otimes \alpha_5^1, \end{aligned} \quad (18)$$

(c) $J^P = 2^+$:

$$\Psi_{C2}^{2^+} = \varphi_C \otimes \alpha_2^2, \quad (19)$$

4. Type D: $\varphi_D = \{(nn\bar{c}\bar{b})^{I=0}\}$ (a) $J^P = 0^+$:

$$\begin{aligned} \Psi_{D1}^{0^+} &= \varphi_D \otimes \alpha_1^0, \\ \Psi_{D2}^{0^+} &= \varphi_D \otimes \alpha_4^0, \end{aligned} \quad (20)$$

(b) $J^P = 1^+$:

$$\begin{aligned} \Psi_{D1}^{1^+} &= \varphi_D \otimes \alpha_1^1, \\ \Psi_{D2}^{1^+} &= \varphi_D \otimes \alpha_2^1, \\ \Psi_{D3}^{1^+} &= \varphi_D \otimes \alpha_6^1, \end{aligned} \quad (21)$$

(c) $J^P = 2^+$:

$$\Psi_D^{2^+} = \varphi_D \otimes \alpha_1^2, \quad (22)$$

5. Type E: $\varphi_E = \{ns\bar{Q}\bar{Q}\}$ (a) $J^P = 0^+$:

$$\begin{aligned} \Psi_{E1}^{0^+} &= \varphi_E \otimes \alpha_2^0, \\ \Psi_{E2}^{0^+} &= \varphi_E \otimes \alpha_3^0, \end{aligned} \quad (23)$$

(b) $J^P = 1^+$:

$$\begin{aligned} \Psi_{E1}^{1^+} &= \varphi_E \otimes \alpha_2^1, \\ \Psi_{E2}^{1^+} &= \varphi_E \otimes \alpha_4^1, \\ \Psi_{E3}^{1^+} &= \varphi_E \otimes \alpha_6^1, \end{aligned} \quad (24)$$

(c) $J^P = 2^+$:

$$\Psi_E^{2^+} = \varphi_E \otimes \alpha_2^2, \quad (25)$$

6. Type F: $\varphi_F = \{ns\bar{c}\bar{b}\}$

$$\Psi_{Fi}^{J^+} = \varphi_F \otimes \alpha_i^J, \quad (26)$$

Diagonalizing the Hamiltonian [Eq. (8)] in these bases, we can obtain the masses and eigenvectors of the doubly heavy tetraquarks.

C. Partial decay rates

Next we consider the strong decay properties of the tetraquarks. There are various methods for studying the tetraquark decays, such as the dimeson decay through the quark interchange model [132–135] and the dibaryon decay through the 3P_0 model [136–139]. These models require the dynamical structure of the hadrons, which is beyond the power of the chromomagnetic model. Here we adopt a simple method to estimate the partial decay ratios of the tetraquark states.

In Sec. II B we have constructed the wave function in the $qq\otimes\bar{q}\bar{q}$ configuration, the tetraquark states are superposition of the bases. The tetraquark states can also be written as the linear superposition of the bases in the $q\bar{q}\otimes q\bar{q}$ configuration (see Appendix A). Normally, the $q\bar{q}$ component in the tetraquark can be either of color-singlet or of color-octet. The former one can easily dissociate into two S -wave mesons in relative S wave, which is called “Okubo-Zweig-Iizuka- (OZI)-superallowed” decays. The recoupling coefficient tell us the overlap between the tetraquark and a particular meson \times meson state. Then we can determine the decay amplitude of the tetraquark into that particular meson \times meson channel. The latter one can only fall apart through the gluon exchange [120, 140]. In this work, we will focus on the “OZI-superallowed” decays.

For each decay mode, the branching fraction is proportional to the square of the coefficient c_i of the corresponding component in the eigenvectors, and also depends on the phase space. For two body decay through L -wave, the partial decay width reads [126, 141]

$$\Gamma_i = \gamma_i \alpha \frac{k^{2L+1}}{m^{2L}} \cdot |c_i|^2, \quad (27)$$

where m is the mass of the initial state, k is the momentum of the final states in the rest frame of the initial state,

α is an effective coupling constant, and γ_i is a quantity determined by the decay dynamics. Generally, γ_i is determined by the spatial wave functions of both initial and final states, which are different for each decay process. In the quark model, the spatial wave functions of the pseudoscalar and vector mesons are the same. Thus for each tetraquark, we have

$$\gamma_{M_1 M_2} = \gamma_{M_1 M_2^*} = \gamma_{M_1^* M_2} = \gamma_{M_1^* M_2^*} \quad (28)$$

where M_i and M_i^* are pseudoscalar and vector mesons respectively. Then we can estimate the partial decay width ratios of the tetraquark states.

III. NUMERICAL RESULTS

A. Parameters

To calculate the tetraquark masses, one needs to estimate the parameters $\{m_{ij}^t, v_{ij}^t\}$. In Ref. [125] we used the meson and baryon masses to extract the parameters $\{m_{q_1 \bar{q}_2}^m, v_{q_1 \bar{q}_2}^m\}$ and $\{m_{q_1 q_2}^b, v_{q_1 q_2}^b\}$. The baryon parameters $\{m_{Q_1 Q_2}^b, v_{Q_1 Q_2}^b\}$ between two heavy quarks cannot be fitted from baryons because of the lack of experimental data. For this reason, we adopted the assumptions

$$\delta a_{q_1 q_2}^{bm} \equiv a_{q_1 q_2}^b - a_{q_1 \bar{q}_2}^m \approx 0 \quad (29)$$

and

$$R_{q_1 q_2}^{bm} \equiv v_{q_1 q_2}^b / v_{q_1 \bar{q}_2}^m = 2/3 \pm 0.30 \quad (30)$$

to estimate them from the meson parameters $\{m_{Q_1 \bar{Q}_2}^m, v_{Q_1 \bar{Q}_2}^m\}$. The resulting parameters are listed in Table I. Since the CM interaction strength v_{ij} 's are inversely proportional to the quark masses, the meson parameters $\{v_{c\bar{c}}, v_{c\bar{b}}, v_{b\bar{b}}\}$ between heavy flavors are quite small. Thus the large uncertainty of the ratio $R_{q_1 q_2}^{bm}$ does not have much effects on the baryon parameters $\{v_{cc}, v_{cb}, v_{bb}\}$ and the mass spectrum of the doubly heavy tetraquarks. As shown in Ref. [125], the introduction of the first assumption makes the difference $\delta m_{q_1 q_2}^{bm} \equiv m_{q_1 q_2}^b - m_{q_1 \bar{q}_2}^m$ separable over the two quarks

$$\delta m_{q_1 q_2}^{bm} \approx \delta m_{q_1}^{bm} + \delta m_{q_2}^{bm} \quad (31)$$

where $\delta m_q^{bm} \equiv m_q^b - m_q^m$ is the difference of the effective quark mass extracted from the baryon and meson. In this way, the ten $\delta m_{q_1 q_2}^{bm}$'s reduce to four δm_q^{bm} 's. Actually, such property can be achieved by a weaker assumption. Namely, we assume that the difference $a_{q_1 q_2}^b - a_{q_1 \bar{q}_2}^m$ is separable over the two quarks

$$a_{q_1 q_2}^b - a_{q_1 \bar{q}_2}^m \approx \delta a_{q_1}^{bm} + \delta a_{q_2}^{bm} \quad (32)$$

Then we have

$$\delta m_{q_1 q_2}^{bm} \approx \delta \tilde{m}_{q_1}^{bm} + \delta \tilde{m}_{q_2}^{bm} \quad (33)$$

where

$$\delta \tilde{m}_q^{bm} \equiv m_q^b - m_q^m + \frac{4}{3} \delta a_q^{bm} = \delta m_q^{bm} + \frac{4}{3} \delta a_q^{bm} \quad (34)$$

which includes the quark mass difference and the differences between color interactions. We again reduce the ten $\delta m_{q_1 q_2}^{bm}$'s into four degrees of freedom. All results are unchanged except that we reinterpret the δm_q^{bm} of Ref. [125] as $\delta \tilde{m}_q^{bm}$ (see Table II or Table VI of Ref. [125]).

Now we consider the tetraquarks. In Ref. [127], we used the following scheme to estimate the masses of the fully heavy tetraquarks

$$m_{q_i q_j}^t \approx m_{q_i q_j}^b, \quad (35)$$

$$m_{q_i \bar{q}_j}^t \approx m_{q_i \bar{q}_j}^m, \quad (36)$$

$$v_{q_i q_j}^t \approx v_{q_i q_j}^b, \quad (37)$$

$$v_{q_i \bar{q}_j}^t \approx v_{q_i \bar{q}_j}^m. \quad (38)$$

Within this scheme, we found that the ground states of the fully heavy tetraquarks are dominated by color-sextet configurations, which is consistent with the dynamical calculations [142, 143]. Nonetheless, this scheme ignores the difference of the spatial configurations between the tetraquarks and the normal hadrons, which will evidently cause large uncertainties [1, 143, 144]. To appreciate the uncertainty, we introduce three additional schemes for comparison (see Table III). The scheme III (IV) differs from the scheme I (II) by

$$v_{q_i \bar{q}_j}^t \approx v_{q_i \bar{q}_j}^m \implies v_{q_i \bar{q}_j}^t \approx v_{q_i q_j}^b. \quad (39)$$

Due to the smallness of v_{qQ}^b and $v_{q\bar{Q}}^m$, the results in scheme I (II) are very similar to those in scheme III (IV). Thus we will focus on the scheme I and scheme II.

B. The $nn\bar{Q}\bar{Q}$ systems

1. The $nn\bar{c}\bar{c}$ and $nn\bar{b}\bar{b}$ tetraquarks

Inserting the parameters into the Hamiltonian, we can determine the tetraquark masses. The masses and eigenvectors of the $nn\bar{Q}\bar{Q}$ tetraquarks are listed in Table IV. Here, we assume that the SU(2) flavor symmetry is exact and denote u, d quarks collectively as n . In the following, we will use $T_i(nn\bar{Q}\bar{Q}, m, I, J^P)$ to represent the $nn\bar{Q}\bar{Q}$ tetraquarks, where the subscript i denotes the particular scheme of the parameters. In Figs 1–2, we plot the relative position of the $nn\bar{Q}\bar{Q}$ tetraquarks and their meson-meson thresholds.

We first consider the $nn\bar{c}\bar{c}$ tetraquarks. The quantum number of its lightest state is $IJ^P = 01^+$, namely the

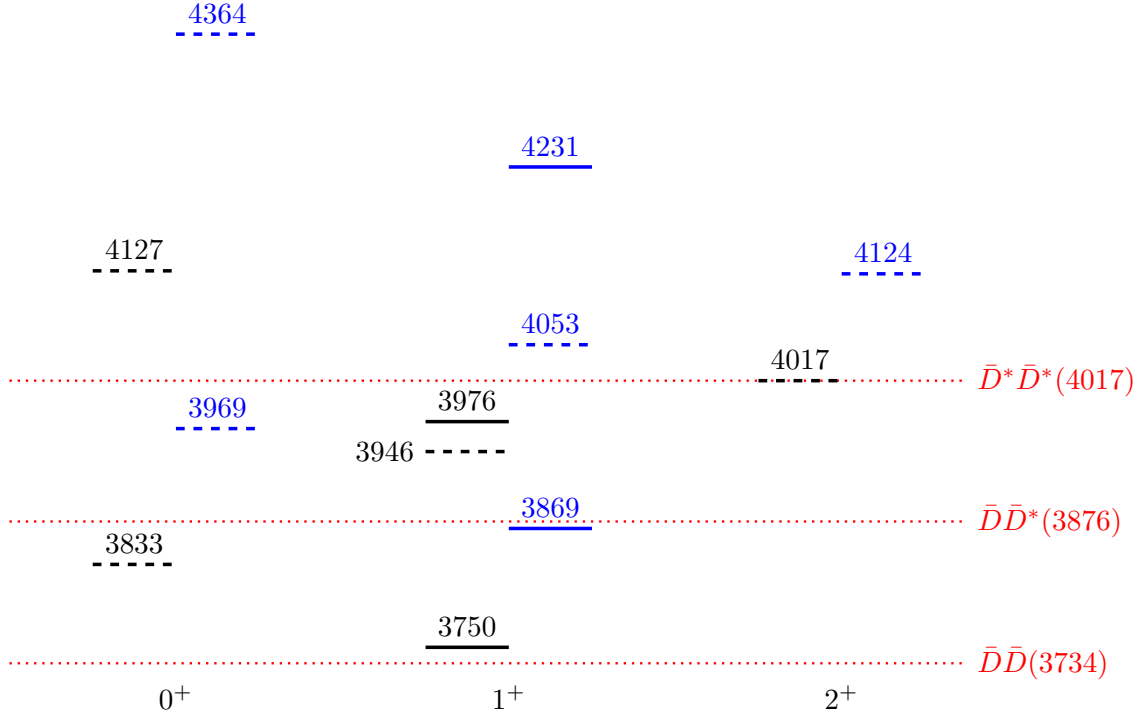
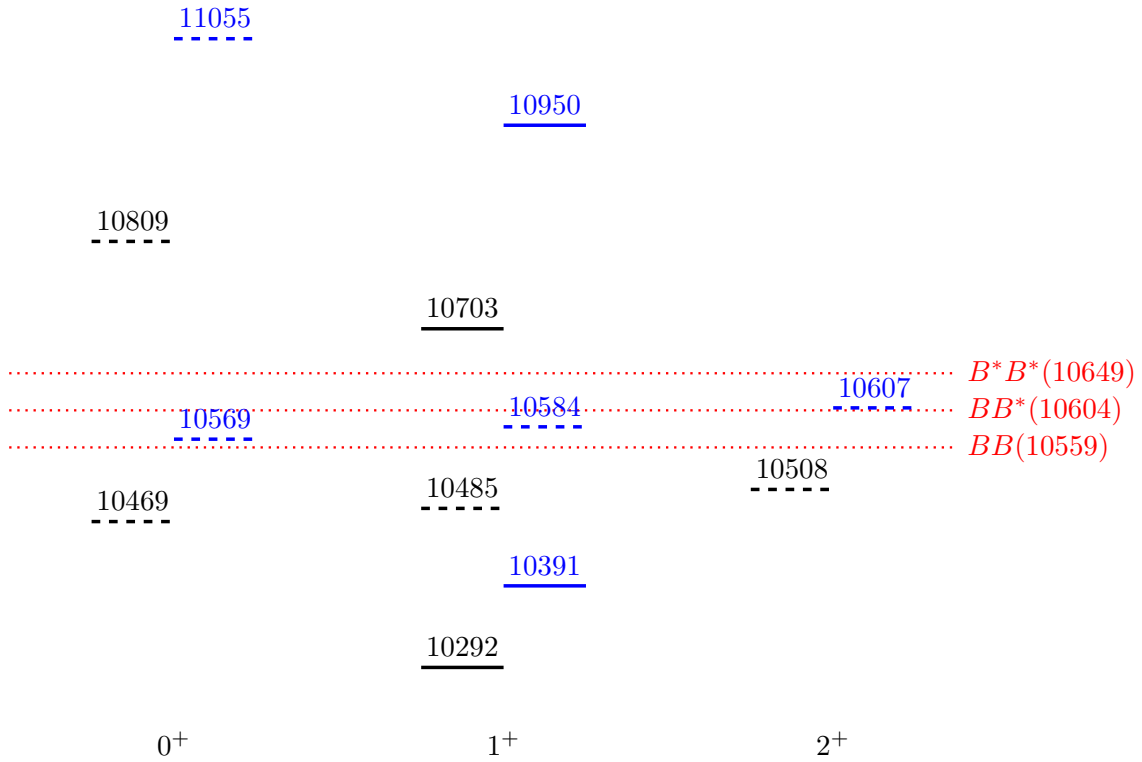
(a) $nn\bar{c}\bar{c}$ states(b) $nn\bar{b}\bar{b}$ states

FIG. 1. Mass spectra of the $I = 0$ (solid) and $I = 1$ (dashed) $nn\bar{c}\bar{c}$ and $nn\bar{b}\bar{b}$ tetraquark states in scheme I (black) and scheme II (blue). The dotted lines indicate various meson-meson thresholds. The masses are all in units of MeV.

TABLE I. Parameters of the $q\bar{q}$ pairs for mesons and of the qq pairs for baryons [125] (in units of MeV).

Parameter	$m_{n\bar{n}}^m$	$m_{n\bar{s}}^m$	$m_{s\bar{s}}^m$	$m_{n\bar{c}}^m$	$m_{s\bar{c}}^m$	$m_{c\bar{c}}^m$	$m_{n\bar{b}}^m$	$m_{s\bar{b}}^m$	$m_{c\bar{b}}^m$	$m_{b\bar{b}}^m$
Value	615.95	794.22	936.40	1973.22	2076.14	3068.53	5313.35	5403.25	6322.27	9444.97
Parameter	$v_{n\bar{n}}^m$	$v_{n\bar{s}}^m$	$v_{s\bar{s}}^m$	$v_{n\bar{c}}^m$	$v_{s\bar{c}}^m$	$v_{c\bar{c}}^m$	$v_{n\bar{b}}^m$	$v_{s\bar{b}}^m$	$v_{c\bar{b}}^m$	$v_{b\bar{b}}^m$
Value	477.92	298.57	249.18	106.01	107.87	85.12	33.89	36.43	47.18	45.98
Parameter	m_{nn}^b	m_{ns}^b	m_{ss}^b	m_{nc}^b	m_{sc}^b	m_{cc}^b	m_{nb}^b	m_{sb}^b	m_{cb}^b	m_{bb}^b
Value	724.85	906.65	1049.36	2079.96	2183.68	3171.51	5412.25	5494.80	6416.07	9529.57
Parameter	v_{nn}^b	v_{ns}^b	v_{ss}^b	v_{nc}^b	v_{sc}^b	v_{cc}^b	v_{nb}^b	v_{sb}^b	v_{cb}^b	v_{bb}^b
Value	305.34	212.75	195.30	62.81	70.63	56.75	19.92	8.47	31.45	30.65

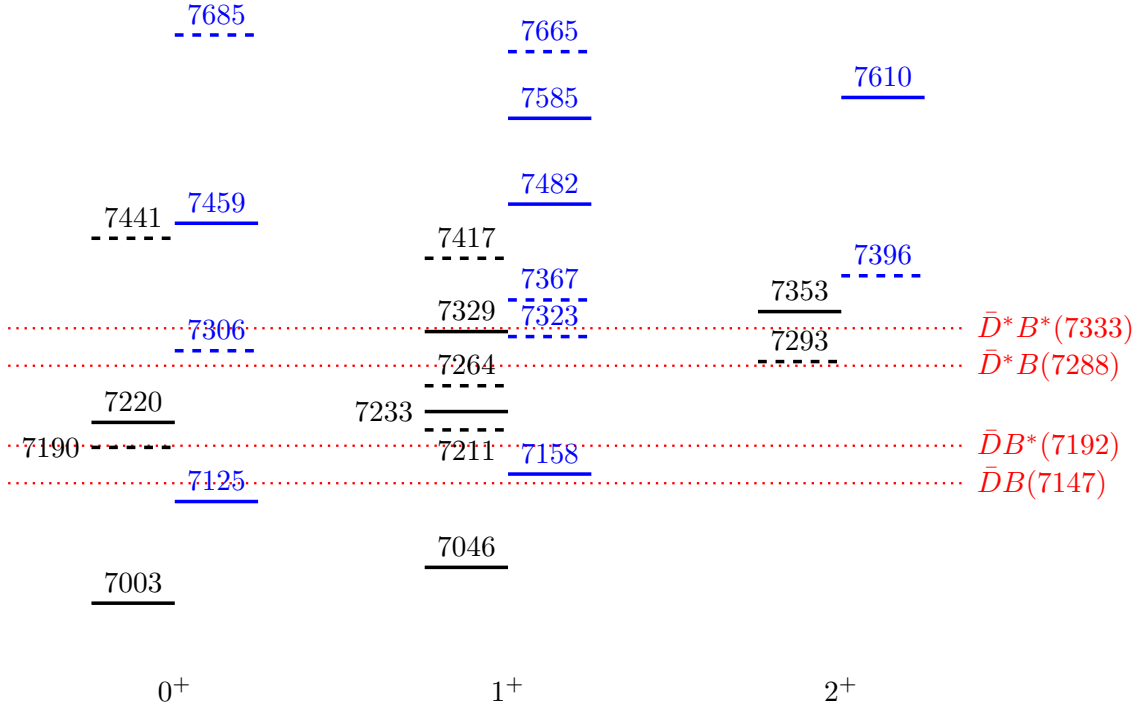
FIG. 2. Mass spectra of the $I = 0$ (solid) and $I = 1$ (dashed) $nn\bar{c}\bar{b}$ tetraquark states in scheme I (black) and scheme II (blue). The dotted lines indicate various meson-meson thresholds. The masses are all in units of MeV.

TABLE II. Values of the difference $\delta\tilde{m}_q^{bm} = m_q^b - m_q^m + \frac{4}{3}\delta a_q^{bm}$ [125] (in units of MeV).

	$\delta\tilde{m}_n^{bm}$	$\delta\tilde{m}_s^{bm}$	$\delta\tilde{m}_c^{bm}$	$\delta\tilde{m}_b^{bm}$
Value	54.94	56.48	51.49	42.30

TABLE III. Possible choices of tetraquark parameters.

	$m_{q_i q_j}^t$	$m_{q_i \bar{q}_j}^t$	$v_{q_i q_j}^t$	$v_{q_i \bar{q}_j}^t$
Scheme I	$m_{q_i q_j}^b$	$m_{q_i \bar{q}_j}^m$	$v_{q_i q_j}^b$	$v_{q_i \bar{q}_j}^m$
Scheme II	$m_{q_i q_j}^b$	$m_{q_i \bar{q}_j}^b$	$v_{q_i q_j}^b$	$v_{q_i \bar{q}_j}^m$
Scheme III	$m_{q_i q_j}^b$	$m_{q_i \bar{q}_j}^m$	$v_{q_i q_j}^b$	$v_{q_i \bar{q}_j}^b$
Scheme IV	$m_{q_i q_j}^b$	$m_{q_i \bar{q}_j}^b$	$v_{q_i q_j}^b$	$v_{q_i \bar{q}_j}^b$

$T_I(nn\bar{c}\bar{c}, 3749.8, 0, 1^+)$ or $T_{II}(nn\bar{c}\bar{c}, 3868.7, 0, 1^+)$ state. The other isoscalar state is $T_I(nn\bar{c}\bar{c}, 3976.1, 0, 1^+)$ or $T_{II}(nn\bar{c}\bar{c}, 4230.8, 0, 1^+)$. We find that the scheme II always gives larger masses than the scheme I. The reason is that the two schemes choose different value of $m_{q_i \bar{q}_j}^t$, which results in different values of the color interaction. More precisely, the difference of the color interaction between the two schemes is

$$\begin{aligned}
\Delta H_C &= H_C^{II} - H_C^I \\
&= -\frac{3}{4} \sum_{i<j} (m_{ij}^{II} - m_{ij}^I) V_{ij}^C \\
&= -\frac{3}{4} \sum_{i\leq 2} \sum_{j>2} \delta m_{ij}^{bm} V_{ij}^C \\
&\approx -\frac{3}{4} \sum_{i\leq 2} \sum_{j>2} (\delta\tilde{m}_i^{bm} + \delta\tilde{m}_j^{bm}) \mathbf{F}_i \cdot \mathbf{F}_j \\
&= \frac{3}{8} \left(\sum_i \delta\tilde{m}_i^{bm} \right) \cdot \left(\sum_{i\leq 2} \mathbf{F}_i \right)^2 \quad (40)
\end{aligned}$$

where in the last line we have ignored the terms proportional to $\sum_i \mathbf{F}_i$. Note that both $|(q_1 q_2)^{6_c} (\bar{q}_3 \bar{q}_4)^{\bar{6}_c}\rangle$ and $|(q_1 q_2)^{\bar{3}_c} (\bar{q}_3 \bar{q}_4)^{3_c}\rangle$ are eigenstates of $(\mathbf{F}_1 + \mathbf{F}_2)^2$, with eigenvalues $10/3$ and $4/3$ respectively. In other words,

$$\langle \Delta H_C \rangle = \begin{cases} \frac{5}{4} \sum_i \delta\tilde{m}_i^{bm}, & \text{for } |(q_1 q_2)^{6_c} (\bar{q}_3 \bar{q}_4)^{\bar{6}_c}\rangle, \\ \frac{1}{2} \sum_i \delta\tilde{m}_i^{bm}, & \text{for } |(q_1 q_2)^{\bar{3}_c} (\bar{q}_3 \bar{q}_4)^{3_c}\rangle. \end{cases} \quad (41)$$

For the $nn\bar{c}\bar{c}$ system, $\sum_i \delta\tilde{m}_i^{bm} = 212.9$ MeV. The ground state $T_I(nn\bar{c}\bar{c}, 3749.8, 0, 1^+)$ is dominated by the color-triplet configuration, and its mass is increased by about 118.9 MeV. While the mass of the color-sextet configuration dominated state $T_I(nn\bar{c}\bar{c}, 3976.1, 0, 1^+)$ is

increased by 254.7 MeV. The deviation from Eq. (41) is caused by the color mixing. In the isovector sector, we have four tetraquark states. They are all above the corresponding S -wave decay channels. It is interesting to note that the $T_{II}(nn\bar{c}\bar{c}, 3868.7, 0, 1^+)$ in scheme II is quite close to the newly observed T_{cc}^+ state.

The $nn\bar{b}\bar{b}$ tetraquarks is very similar to the $nn\bar{c}\bar{c}$ tetraquarks. Its lightest state also have quantum number $IJ^P = 01^+$, namely the $T_I(nn\bar{b}\bar{b}, 10291.6, 0, 1^+)$ or $T_{II}(nn\bar{b}\bar{b}, 10390.9, 0, 1^+)$. In both schemes, this state lies below the BB threshold and is stable against strong decays. In scheme I, the $T_I(nn\bar{b}\bar{b}, 10468.9, 1, 0^+)$, $T_I(nn\bar{b}\bar{b}, 10485.3, 1, 1^+)$ and $T_I(nn\bar{b}\bar{b}, 10507.9, 1, 2^+)$ also lie below the the BB threshold. But they are not stable in scheme II. Thus we cannot draw a definite conclusion.

Besides the masses, the eigenvectors also help understand the nature of the tetraquarks. Within the four possible quantum numbers, the $IJ^P = 10^+$ one and the $IJ^P = 01^+$ one are of particular interest because they both have two possible color configurations, namely the color-sextet $|(qq)^{6_c} \otimes (\bar{Q}\bar{Q})^{\bar{6}_c}\rangle$ and color-triplet $|(qq)^{\bar{3}_c} \otimes (\bar{Q}\bar{Q})^{3_c}\rangle$. For simplicity, we denote them as $6_c \otimes \bar{6}_c$ and $\bar{3}_c \otimes 3_c$. As pointed out by Wang *et al.* [142], there are two competing effects in determining whether the $6_c \otimes \bar{6}_c$ or $\bar{3}_c \otimes 3_c$ dominates the tetraquark's ground state. In the one-gluon-exchange (OGE) model, the color interactions in color-triplet diquark are attractive, while those in color-sextet diquark are repulsive. On the other hand, the attractions between 6_c diquark and $\bar{6}_c$ antiquark and between the $\bar{3}_c \otimes 3_c$ counterpart are both attractive, and the former one is much stronger. The authors of Refs. [127, 142, 143] found that the color-sextet configuration has more net attractions for most fully heavy tetraquarks. Thus the ground states contain more color-sextet components than the color-triplet one. The only exception is the $cc\bar{b}\bar{b}$ tetraquark in model II of Ref [142], whose ground state has 53% of the $\bar{3}_c \otimes 3_c$ component. It is also interesting to note that, when the mass ratio between quarks and antiquarks deviates from one, the color-triplet configuration becomes more important in the ground states. For example, Ref. [127] found that the $T(bb\bar{b}\bar{b}, 18836.1, 0^{++})$ and $T(cc\bar{c}\bar{c}, 6044.9, 0^{++})$ have 18.5% and 30.5% of the $\bar{3}_c \otimes 3_c$ components, while the $T(cc\bar{b}\bar{b}, 12596.3, 0^{++})$ has 48.4%. This tendency also exists in the doubly heavy tetraquarks. As shown in Table IV, the $\bar{3}_c \otimes 3_c$ components become dominant in ground states of the $nn\bar{Q}\bar{Q}$ tetraquarks. This phenomenon can also be explained by the color interaction Hamiltonian,

$$\begin{aligned}
&\langle H_C (nn\bar{Q}\bar{Q}) \rangle \\
&= -\frac{3}{4} \left\langle m_{nn}^t V_{12}^C + m_{Q\bar{Q}}^t V_{34}^C + m_{n\bar{Q}}^t (V_{13}^C + V_{24}^C + V_{14}^C + V_{23}^C) \right\rangle \\
&= -\frac{3}{4} \left\langle m_{n\bar{Q}}^t \sum_{i<j} V_{ij}^C + 2\delta m (V_{12}^C + V_{34}^C) \right\rangle \\
&= 2m_{n\bar{Q}}^t - \frac{3}{2} \delta m \langle V_{12}^C + V_{34}^C \rangle
\end{aligned}$$

TABLE IV. Masses and eigenvectors of the $nn\bar{c}\bar{c}$, $nn\bar{b}\bar{b}$ and $nn\bar{c}\bar{b}$ tetraquarks. The masses are all in units of MeV.

System	J^P	Scheme I		Scheme II	
		Mass	Eigenvector	Mass	Eigenvector
$(nn\bar{c}\bar{c})^{I=1}$	0^+	3833.2	{0.515, 0.857}	3969.2	{0.350, 0.937}
		4127.4	{0.857, -0.515}	4364.9	{0.937, -0.350}
	1^+	3946.4	{1}	4053.2	{1}
	2^+	4017.1	{1}	4123.8	{1}
$(nn\bar{c}\bar{c})^{I=0}$	1^+	3749.8	{0.354, -0.935}	3868.7	{0.212, -0.977}
		3976.1	{0.935, 0.354}	4230.8	{0.977, 0.212}
$(nn\bar{b}\bar{b})^{I=1}$	0^+	10468.8	{0.123, 0.992}	10569.3	{0.086, 0.996}
		10808.9	{0.992, -0.123}	11054.6	{0.996, -0.086}
	1^+	10485.3	{1}	10584.2	{1}
	2^+	10507.9	{1}	10606.8	{1}
$(nn\bar{b}\bar{b})^{I=0}$	1^+	10291.6	{0.058, -0.998}	10390.9	{0.043, -0.999}
		10703.4	{0.998, 0.058}	10950.3	{0.999, 0.043}
$(nn\bar{c}\bar{b})^{I=1}$	0^+	7189.5	{0.366, 0.931}	7305.6	{0.232, 0.973}
		7440.9	{0.931, -0.366}	7684.7	{0.973, -0.232}
	1^+	7211.0	{-0.311, -0.648, 0.696}	7322.5	{-0.180, -0.687, 0.704}
		7264.2	{-0.048, 0.742, 0.669}	7367.3	{-0.029, 0.719, 0.694}
		7417.0	{0.949, -0.175, 0.262}	7665.1	{0.983, -0.104, 0.150}
	2^+	7293.2	{1}	7396.0	{1}
$(nn\bar{c}\bar{b})^{I=0}$	0^+	7003.4	{0.440, 0.898}	7124.6	{0.266, 0.964}
		7220.3	{0.898, -0.440}	7459.0	{0.964, -0.266}
	1^+	7046.2	{0.228, -0.219, 0.949}	7158.0	{0.122, -0.133, 0.984}
		7232.9	{0.899, -0.327, -0.292}	7482.4	{0.910, -0.381, -0.165}
		7329.3	{-0.374, -0.919, -0.122}	7584.9	{-0.397, -0.915, -0.074}
	2^+	7353.2	{1}	7610.3	{1}

TABLE V. The eigenvectors of the $nn\bar{c}\bar{c}$ tetraquark states in the $n\bar{c}\otimes n\bar{c}$ configuration. The masses are all in units of MeV.

System	J^P	Scheme I				Scheme II				
		Mass	$\bar{D}^*\bar{D}^*$	$\bar{D}^*\bar{D}$	$\bar{D}\bar{D}^*$	$\bar{D}\bar{D}$	Mass	$\bar{D}^*\bar{D}^*$	$\bar{D}^*\bar{D}$	$\bar{D}\bar{D}^*$
$(nn\bar{c}\bar{c})^{I=1}$	0^+	3833.2	0.116		0.639	3969.2	-0.023			0.611
		4127.4	0.755		0.093	4364.9	0.763			0.207
	1^+	3946.4	0	0.408	0.408	4053.2	0	0.408	0.408	
	2^+	4017.1	0.577			4123.8	0.577			
$(nn\bar{c}\bar{c})^{I=0}$	1^+	3749.8	-0.177	0.415	-0.415	3868.7	-0.277	0.369	-0.369	
		3976.1	0.685	0.280	-0.280	4230.8	0.651	0.338	-0.338	

TABLE VI. The values of $k \cdot |c_i|^2$ for the $nn\bar{c}\bar{c}$ tetraquarks (in unit of MeV).

System	J^P	Scheme I			Scheme II				
		Mass	$\bar{D}^*\bar{D}^*$	$\bar{D}\bar{D}^*$	$\bar{D}\bar{D}$	Mass	$\bar{D}^*\bar{D}^*$	$\bar{D}\bar{D}^*$	$\bar{D}\bar{D}$
$(nn\bar{c}\bar{c})^{I=1}$	0^+	3833.2	×		176.4	3969.2	×		251.3
		4127.4	270.0		7.6	4364.9	497.6		48.5
	1^+	3946.4		61.9		4053.2		98.8	
	2^+	4017.1	×			4123.8	155.3		
$(nn\bar{c}\bar{c})^{I=0}$	1^+	3749.8	×	×		3868.7	×	×	
		3976.1	×	34.7		4230.8	281.1	96.8	

TABLE VII. The partial width ratios for the $nn\bar{c}\bar{c}$ tetraquarks. For each state, we choose one mode as the reference channel, and the partial width ratios of the other channels are calculated relative to this channel. The masses are all in unit of MeV.

System	J^P	Scheme I			Scheme II				
		Mass	$\bar{D}^*\bar{D}^*$	$\bar{D}\bar{D}^*$	$\bar{D}\bar{D}$	Mass	$\bar{D}^*\bar{D}^*$	$\bar{D}\bar{D}^*$	$\bar{D}\bar{D}$
$(nn\bar{c}\bar{c})^{I=1}$	0^+	3833.2	×		1	3969.2	×		1
		4127.4	35.7		1	4364.9	10.3		1
	1^+	3946.4		1		4053.2		1	
	2^+	4017.1	×			4123.8	1		
$(nn\bar{c}\bar{c})^{I=0}$	1^+	3749.8	×	×		3868.7	×	×	
		3976.1	×	1		4230.8	1.5	1	

TABLE VIII. The eigenvectors of the $nn\bar{b}\bar{b}$ tetraquark states in the $n\bar{b}\otimes n\bar{b}$ configuration. The masses are all in units of MeV.

System	J^P	Scheme I				Scheme II					
		Mass	B^*B^*	B^*B	BB^*	BB	Mass	B^*B^*	B^*B	BB^*	BB
$(nn\bar{b}\bar{b})^{I=1}$	0^+	10468.8	-0.200			0.546	10569.3	-0.227			0.533
		10808.9	0.737			0.344	11054.6	0.729			0.364
	1^+	10485.3	0	0.408	0.408		10584.2	0	0.408	0.408	
2^+	10507.9	0.577				10606.8	0.577				
$(nn\bar{b}\bar{b})^{I=0}$	1^+	10291.6	-0.374	0.312	-0.312		10390.9	-0.383	0.306	-0.306	
		10703.4	0.600	0.391	-0.391		10950.3	0.594	0.395	-0.395	

TABLE IX. The values of $k \cdot |c_i|^2$ for the $nn\bar{b}\bar{b}$ tetraquarks (in unit of MeV).

System	J^P	Scheme I				Scheme II			
		Mass	B^*B^*	BB^*	BB	Mass	B^*B^*	BB^*	BB
$(nn\bar{b}\bar{b})^{I=1}$	0^+	10468.8	×		×	10569.3	×		66.5
		10808.9	503.0		136.5	11054.6	788.7		216.6
	1^+	10485.3		×		10584.2		×	
	2^+	10507.9	×			10606.8	×		
$(nn\bar{b}\bar{b})^{I=0}$	1^+	10291.6	×	×		10390.9	×	×	
		10703.4	193.6	111.0		10950.3	450.3	213.6	

TABLE X. The partial width ratios for the $nn\bar{b}\bar{b}$ tetraquarks. For each state, we choose one mode as the reference channel, and the partial width ratios of the other channels are calculated relative to this channel. The masses are all in unit of MeV.

System	J^P	Scheme I				Scheme II			
		Mass	B^*B^*	BB^*	BB	Mass	B^*B^*	BB^*	BB
$(nn\bar{b}\bar{b})^{I=1}$	0^+	10468.8	×		×	10569.3	×		1
		10808.9	3.7		1	11054.6	3.6		1
	1^+	10485.3		×		10584.2		×	
	2^+	10507.9	×			10606.8	×		
$(nn\bar{b}\bar{b})^{I=0}$	1^+	10291.6	×	×		10390.9	×	×	
		10703.4	0.9	1		10950.3	1.1	1	

TABLE XI. The eigenvectors of the $nn\bar{c}\bar{b}$ tetraquark states in the $n\bar{c}\otimes n\bar{b}$ configuration. The masses are all in units of MeV.

System	J^P	Scheme I				Scheme II					
		Mass	\bar{D}^*B^*	\bar{D}^*B	$\bar{D}B^*$	$\bar{D}B$	Mass	\bar{D}^*B^*	\bar{D}^*B	$\bar{D}B^*$	$\bar{D}B$
$(nn\bar{c}\bar{b})^{I=1}$	0^+	7189.5	-0.010			0.615	7305.6	-0.116			0.581
		7440.9	0.764			0.197	7684.7	0.755			0.281
	1^+	7211.0	0.104	0.063	-0.592		7322.5	0.184	-0.004	-0.557	
		7264.2	0.245	0.515	0.090		7367.3	0.266	0.506	0.081	
2^+	7417.0	0.655	-0.383	0.241		7665.1	0.629	-0.401	0.316		
	7293.2	0.577				7396.0	0.577				
$(nn\bar{c}\bar{b})^{I=0}$	0^+	7003.4	0.269			0.570	7124.6	0.374			0.466
		7220.3	-0.587			0.508	7459.0	-0.526			0.605
	1^+	7046.2	0.261	-0.231	0.495		7158.0	0.325	-0.268	0.409	
		7232.9	-0.308	0.469	0.568		7482.4	-0.287	0.417	0.633	
2^+	7329.3	-0.580	-0.556	0.124		7584.9	-0.559	-0.581	0.123		
	7353.2	0.817				7610.3	0.817				

TABLE XII. The values of $k \cdot |c_i|^2$ for the $nn\bar{c}\bar{b}$ tetraquarks (in unit of MeV).

System	J^P	Scheme I				Scheme II					
		Mass	\bar{D}^*B^*	\bar{D}^*B	$\bar{D}B^*$	$\bar{D}B$	Mass	\bar{D}^*B^*	\bar{D}^*B	$\bar{D}B^*$	$\bar{D}B$
$(nn\bar{c}\bar{b})^{I=1}$	0^+	7189.5	×			130.4	7305.6	×			226.3
		7440.9	329.3			35.6	7684.7	590.5			99.9
	1^+	7211.0	×	×	80.7		7322.5	×	0.004	188.4	
		7264.2	×	×	3.7		7367.3	22.4	123.6	4.7	
		7417.0	213.2	90.8	46.4		7665.1	397.6	172.5	117.9	
2^+	7293.2	×				7396.0	143.3				
$(nn\bar{c}\bar{b})^{I=0}$	0^+	7003.4	×			×	7124.6	×			×
		7220.3	×			117.0	7459.0	169.3			347.6
	1^+	7046.2	×	×	×		7158.0	×	×	×	
		7232.9	×	×	109.1		7482.4	55.0	132.7	367.1	
		7329.3	×	107.5	9.6		7584.9	271.9	320.1	16.2	
2^+	7353.2	161.3				7610.3	610.5				

TABLE XIII. The partial width ratios for the $nn\bar{c}\bar{b}$ tetraquarks. For each state, we choose one mode as the reference channel, and the partial width ratios of the other channels are calculated relative to this channel. The masses are all in unit of MeV.

System	J^P	Scheme I				Scheme II					
		Mass	\bar{D}^*B^*	\bar{D}^*B	$\bar{D}B^*$	$\bar{D}B$	Mass	\bar{D}^*B^*	\bar{D}^*B	$\bar{D}B^*$	$\bar{D}B$
$(nn\bar{c}\bar{b})^{I=1}$	0^+	7189.5	×			1	7305.6	×			1
		7440.9	9.2			1	7684.7	5.9			1
	1^+	7211.0	×	×	1		7322.5	×	0.00002	1	
		7264.2	×	×	1		7367.3	4.8	26.5	1	
		7417.0	4.6	2.0	1		7665.1	3.4	1.5	1	
2^+	7293.2	×				7396.0	1				
$(nn\bar{c}\bar{b})^{I=0}$	0^+	7003.4	×			×	7124.6	×			×
		7220.3	×			1	7459.0	0.5			1
	1^+	7046.2	×	×	×		7158.0	×	×	×	
		7232.9	×	×	1		7482.4	0.1	0.4	1	
		7329.3	×	11.2	1		7584.9	16.8	19.7	1	
2^+	7353.2	1				7610.3	1				

$$= 2m_{n\bar{Q}}^t + \delta m \begin{pmatrix} -1 & 0 \\ 0 & +2 \end{pmatrix} \quad (42)$$

where we have expanded the Hamiltonian in the bases $\{|(n_1 n_2)_0^6 (\bar{Q}_3 \bar{Q}_4)_0^6\rangle, |(n_1 n_2)_1^3 (\bar{Q}_3 \bar{Q}_4)_1^3\rangle\}$ in the last line and

$$\delta m = \frac{1}{2} \left(\frac{m_{nn}^t + m_{QQ}^t}{2} - m_{n\bar{Q}}^t \right) \quad (43)$$

Taking scheme I as an example, we have

$$\delta m (nn\bar{c}\bar{c}) = -12.52 \text{ MeV}, \quad (44)$$

$$\delta m (n\bar{m}b\bar{b}) = -93.07 \text{ MeV}, \quad (45)$$

while for the fully heavy tetraquarks

$$\delta m (bb\bar{b}\bar{b}) = +42.30 \text{ MeV}, \quad (46)$$

$$\delta m (cc\bar{c}\bar{c}) = +51.49 \text{ MeV}, \quad (47)$$

$$\delta m (c\bar{c}b\bar{b}) = +15.15 \text{ MeV}. \quad (48)$$

As the ratios $m_{\bar{q}}/m_q$'s increase, the $\bar{3}_c \otimes 3_c$ components become more important in the ground states.

Another interesting conclusion from the Hamiltonian is that the color interaction does not mix the $6_c \otimes \bar{6}_c$ and $\bar{3}_c \otimes 3_c$ configurations. Actually, this conclusion applies for all S -wave tetraquarks with $q_1 = q_2$ or $\bar{q}_3 = \bar{q}_4$. Let's consider the matrix element of color interaction $\langle \alpha | H_{CE} | \beta \rangle$. Note that the color interaction is independent of the spin operator, and thus is a rank-0 tensor in the $q_1 q_2$ spin space. Its matrix elements over different $q_1 q_2$ spin states always vanish. If $q_1 = q_2$, the Pauli principle further renders the matrix elements vanish unless the bases α and β possess the same color symmetry over $q_1 q_2$. The same argument works for $\bar{q}_3 \bar{q}_4$ as well. In summary, the color interaction does not mix the $6_c \otimes \bar{6}_c$ and $\bar{3}_c \otimes 3_c$ color configurations if $q_1 = q_2$ or $\bar{q}_3 = \bar{q}_4$.

Next we consider their decay properties. For the decays of the tetraquark states in this work, the $(k/m)^2$'s are all of $\mathcal{O}(10^{-2})$ or even smaller. All higher wave decays are suppressed. Thus we will only consider the S -wave decays in this work. First we transform the wave function of $nn\bar{Q}\bar{Q}$ tetraquarks into the $n\bar{Q} \otimes n\bar{Q}$ configuration. Then we can calculate the $k \cdot |c_i|^2$'s and partial decay width ratios. The corresponding results are listed in Tables V-X. Note that the two schemes give very similar results, we will mainly focus on the scheme I in the following. In the isovector sector, the $nn\bar{c}\bar{c}$ tetraquarks are mostly above the S -wave decay channels, thus are wide states. Depending on the schemes, the $J^P = 2^+$ state may lie on or above the $\bar{D}^* \bar{D}^*$ threshold. Namely the $T_I(nn\bar{c}\bar{c}, 4017.1, 1, 2^+)$ or $T_{II}(nn\bar{c}\bar{c}, 4123.8, 1, 2^+)$. A firm conclusion requires more detailed studies. The $T_I(nn\bar{c}\bar{c}, 4127.4, 1, 0^+)$ can decay into both $\bar{D}\bar{D}$ and $\bar{D}^* \bar{D}^*$ channels, with partial decay width ratio

$$\Gamma_{\bar{D}^* \bar{D}^*} : \Gamma_{\bar{D}\bar{D}} \sim 37.5. \quad (49)$$

Thus the $\bar{D}^* \bar{D}^*$ mode is dominant. In the isoscalar sector, the $T_I(nn\bar{c}\bar{c}, 3749.8, 0, 1^+)$ lies below the $\bar{D}\bar{D}^*$ threshold, thus it is a narrow state. However, this state lies above the $\bar{D}\bar{D}$ threshold, so it can decay radiatively into the $\bar{D}\bar{D}\gamma$ final states. The $T_I(nn\bar{c}\bar{c}, 3976.1, 0, 1^+)$ is wide because it lies above the $\bar{D}\bar{D}^*$ and $\bar{D}^* \bar{D}^*$ thresholds. The $T_I(n\bar{m}b\bar{b}, 10808.9, 1, 0^+)$ and $T_I(n\bar{m}b\bar{b}, 10703.4, 0, 1^+)$ lie above all the corresponding S -wave decay channel. Their partial decay width ratios are

$$\frac{\Gamma[T_I(n\bar{m}b\bar{b}, 10808.9, 1, 0^+) \rightarrow B^* B^*]}{\Gamma[T_I(n\bar{m}b\bar{b}, 10808.9, 1, 0^+) \rightarrow BB]} \sim 3.7 \quad (50)$$

and

$$\frac{\Gamma[T_I(n\bar{m}b\bar{b}, 10703.4, 0, 1^+) \rightarrow B^* B^*]}{\Gamma[T_I(n\bar{m}b\bar{b}, 10703.4, 0, 1^+) \rightarrow BB]} \sim 0.9 \quad (51)$$

respectively. Other $n\bar{m}b\bar{b}$ tetraquarks are all narrow states.

2. The $nn\bar{c}\bar{b}$ tetraquark

Next we consider the $nn\bar{c}\bar{b}$ tetraquark. We list the masses and eigenvectors of these states in Table IV. Their relative position and possible decay channels are plotted in Fig. 2. There are two possible stable $nn\bar{c}\bar{b}$ tetraquark states. The first state is $T_I(nn\bar{c}\bar{b}, 7003.4, 0, 0^+)$, which lies below the $\bar{D}B$ threshold by more than 100 MeV. Even in scheme II, this state is about 20 MeV below the threshold. The second state is $T_I(nn\bar{c}\bar{b}, 7046.2, 0, 1^+)$. It is about 100 MeV lighter than the $\bar{D}B$ threshold. However, this state lies above the threshold in scheme II. Nonetheless, it lies below its S -wave decay mode $\bar{D}B^*$, thus should be a narrow state.

Since the two antiquarks do not have to obey the Pauli principle, we have much bigger number of states than the $nn\bar{c}\bar{c}/n\bar{m}b\bar{b}$ cases. For each isospin, we have two 0^+ states, three 1^+ states and one 2^+ state. From Table IV, we see that for each possible quantum number, the lower mass states are dominated by color-triplet configurations, while the color-sextet configurations are more important in the higher mass states. For example, the two stable states $T_I(nn\bar{c}\bar{b}, 7003.4, 0, 0^+)$ and $T_I(nn\bar{c}\bar{b}, 7046.2, 0, 1^+)$ have 80.6% and 90.0% of $\bar{3}_c \otimes 3_c$ components respectively. This can be explained by the color interaction

$$\langle H_C (nn\bar{c}\bar{b}) \rangle = m_{n\bar{c}} + m_{n\bar{b}} - \frac{3}{2} \delta m' \langle V_{12}^C + V_{34}^C \rangle \quad (52)$$

where

$$\begin{aligned} \delta m' &= \frac{1}{4} (m_{nn} + m_{cb} - m_{n\bar{c}} - m_{n\bar{b}}) \\ &= -36.41 \text{ MeV} \end{aligned} \quad (53)$$

Note that both $6_c \otimes \bar{6}_c$ and $\bar{3}_c \otimes 3_c$ configurations are eigenstates of $V_{12}^C + V_{34}^C$, with eigenvalues $2/3$ and $-4/3$ respectively. The negative value of $\delta m'$ indicates that the color interaction favors the $\bar{3}_c \otimes 3_c$ configuration.

In Table XI, we transform the $nn\bar{c}\bar{b}$ tetraquarks into the $n\bar{c}\otimes n\bar{b}$ configuration. Then we calculate the values of $k \cdot |c_i|^2$ and relative partial decay widths, as shown in Tables XII–XIII. Besides the two stable states discussed above, two heavier isoscalar states $T_I(nn\bar{c}\bar{b}, 7220.3, 0, 0^+)$ and $T_I(nn\bar{c}\bar{b}, 7232.9, 0, 1^+)$ are above the $\bar{D}B^*$, while $T_I(nn\bar{c}\bar{b}, 7329.3, 0, 1^+)$ can decay into both \bar{D}^*B and $\bar{D}B^*$ modes, with relative width

$$\Gamma_{\bar{D}^*B} : \Gamma_{\bar{D}B^*} \sim 11.2 : 1 \quad (54)$$

In the isovector sector, the lower 0^+ state can only decay into $\bar{D}B$ mode, while the higher one can also decay into \bar{D}^*B^* mode. All 1^+ states can decay into $\bar{D}B^*$ in S -wave, while only the highest one can decay into \bar{D}^*B and \bar{D}^*B^* modes, with partial decay rates

$$\Gamma_{\bar{D}^*B^*} : \Gamma_{\bar{D}^*B} : \Gamma_{\bar{D}B^*} \sim 4.6 : 2.0 : 1 \quad (55)$$

There is no doubt that the current results rely on the mass estimation. In scheme II, the higher masses allow the states to have more decay modes. Yet we find that the partial decay width ratios are quite stable in the two schemes.

C. The $ss\bar{Q}\bar{Q}$ systems

We list the numerical results of the $ss\bar{Q}\bar{Q}$ in Table XIV–XXIII. We also plot the relative position and possible decay channels in Figs. 3–4. The pattern of the mass spectrum is very similar to that of the $nn\bar{Q}\bar{Q}$ tetraquarks with isospin $I = 1$.

First we focus on the $ss\bar{c}\bar{c}$ tetraquarks. The ground state is $T_I(ss\bar{c}\bar{c}, 4043.7, 0^+)$. It can decay into $\bar{D}_s\bar{D}_s$ in S -wave, and thus might be a wide state. The most heavy state $T_I(ss\bar{c}\bar{c}, 4311.1, 0^+)$ lies above the $\bar{D}_s^*\bar{D}_s^*$ threshold. It decays into $\bar{D}_s\bar{D}_s$ and $\bar{D}_s^*\bar{D}_s^*$ modes with the ratios

$$\frac{\Gamma[T_I(ss\bar{c}\bar{c}, 4311.1, 0^+) \rightarrow \bar{D}_s\bar{D}_s]}{\Gamma[T_I(ss\bar{c}\bar{c}, 4311.1, 0^+) \rightarrow \bar{D}_s^*\bar{D}_s^*]} \sim 0.0008. \quad (56)$$

Thus the $\bar{D}_s^*\bar{D}_s^*$ mode is dominant. The other two state $T_I(ss\bar{c}\bar{c}, 4192.6, 1^+)$ and $T_I(ss\bar{c}\bar{c}, 4264.5, 2^+)$ can decay into $\bar{D}_s\bar{D}_s^*$ and $\bar{D}_s^*\bar{D}_s^*$ modes respectively.

Next we turn to the $ss\bar{b}\bar{b}$ tetraquarks. In scheme I, the $T_I(ss\bar{b}\bar{b}, 10697.1, 0^+)$ and $T_I(ss\bar{b}\bar{b}, 10718.2, 1^+)$ lie below the B_sB_s threshold, and the $T_I(ss\bar{b}\bar{b}, 10742.5, 2^+)$ lies just above the B_sB_s threshold, which suggests that they are stable states. However, they become heavier than their S -wave decay channels in scheme II. A detailed study with dynamical model, or experimental researches, is required to distinguish which of the two schemes gives better description of the $ss\bar{b}\bar{b}$ tetraquarks. In both schemes, the three states are dominated by $\bar{3}_c \otimes 3_c$ configuration. Actually, their wave functions are nearly the same, except that they have different total spin, which is the reason for their different masses. The highest state can decay into B_sB_s and $B_s^*B_s^*$ modes, with

nearly identical partial width ratios

$$\frac{\Gamma[T_I(ss\bar{b}\bar{b}, 10928.8, 0^+) \rightarrow B_s^*B_s^*]}{\Gamma[T_I(ss\bar{b}\bar{b}, 10928.8, 0^+) \rightarrow B_sB_s]} \sim 4.4 \quad (57)$$

and

$$\frac{\Gamma[T_{II}(ss\bar{b}\bar{b}, 11154.3, 0^+) \rightarrow B_s^*B_s^*]}{\Gamma[T_{II}(ss\bar{b}\bar{b}, 11154.3, 0^+) \rightarrow B_sB_s]} \sim 4.1. \quad (58)$$

From Fig. 4, we see that the $ss\bar{c}\bar{b}$ tetraquarks are all above the S -wave decay channels and are probably broad states. Among them, the $T_I(ss\bar{c}\bar{b}, 7534.3, 2^+)$ is slightly above the $\bar{D}_s^*B_s^*$. Its decay width may be relatively narrow. We also calculate the partial decay width ratios of the $ss\bar{c}\bar{b}$ tetraquarks. It is interesting that some of the ratios are different in the two schemes. For example, in scheme I

$$\frac{\Gamma[T_I(ss\bar{c}\bar{b}, 7597.3, 0^+) \rightarrow \bar{D}_s^*B_s^*]}{\Gamma[T_I(ss\bar{c}\bar{b}, 7597.3, 0^+) \rightarrow \bar{D}_sB_s]} \sim 63.2 \quad (59)$$

and in scheme II

$$\frac{\Gamma[T_I(ss\bar{c}\bar{b}, 7818.8, 0^+) \rightarrow \bar{D}_s^*B_s^*]}{\Gamma[T_I(ss\bar{c}\bar{b}, 7818.8, 0^+) \rightarrow \bar{D}_sB_s]} \sim 9.1, \quad (60)$$

which can be used to distinguish the two schemes.

D. The $ns\bar{Q}\bar{Q}$ systems

We list the masses and wave functions of the $ns\bar{Q}\bar{Q}$ in Table XXIV. The ground states of the $ns\bar{c}\bar{c}$ and $ns\bar{b}\bar{b}$ tetraquarks are both of 1^+ . They are strange counterparts of the $IJ^P = 01^+ nn\bar{Q}\bar{Q}$ tetraquarks. Among them, the $T_I(ns\bar{c}\bar{c}, 3919.0, 1^+)$ lies above the $\bar{D}\bar{D}_s$ threshold, while the $T_I(ns\bar{b}\bar{b}, 10473.1, 1^+)$ lies deeply below the BB_s threshold. In scheme II, the former one lies above its S -wave decay channels $\bar{D}^*\bar{D}_s$ and $\bar{D}\bar{D}_s^*$, while the latter one is still stable. We hope the future experiment can reach for this state.

The last class of the doubly heavy tetraquarks is the $ns\bar{c}\bar{b}$ system. It is composed of four different quarks. Similar to the $nn\bar{c}\bar{b}$ tetraquarks, the ground state of the $ns\bar{c}\bar{b}$ tetraquarks has quantum number 0^+ . Depending on the scheme used, it may be a stable state. A full dynamical quark model study is needed to have a better understanding of these states.

We also study the decay properties of the $ns\bar{Q}\bar{Q}$ tetraquarks, which can be found in Tables XXV–XXXIV.

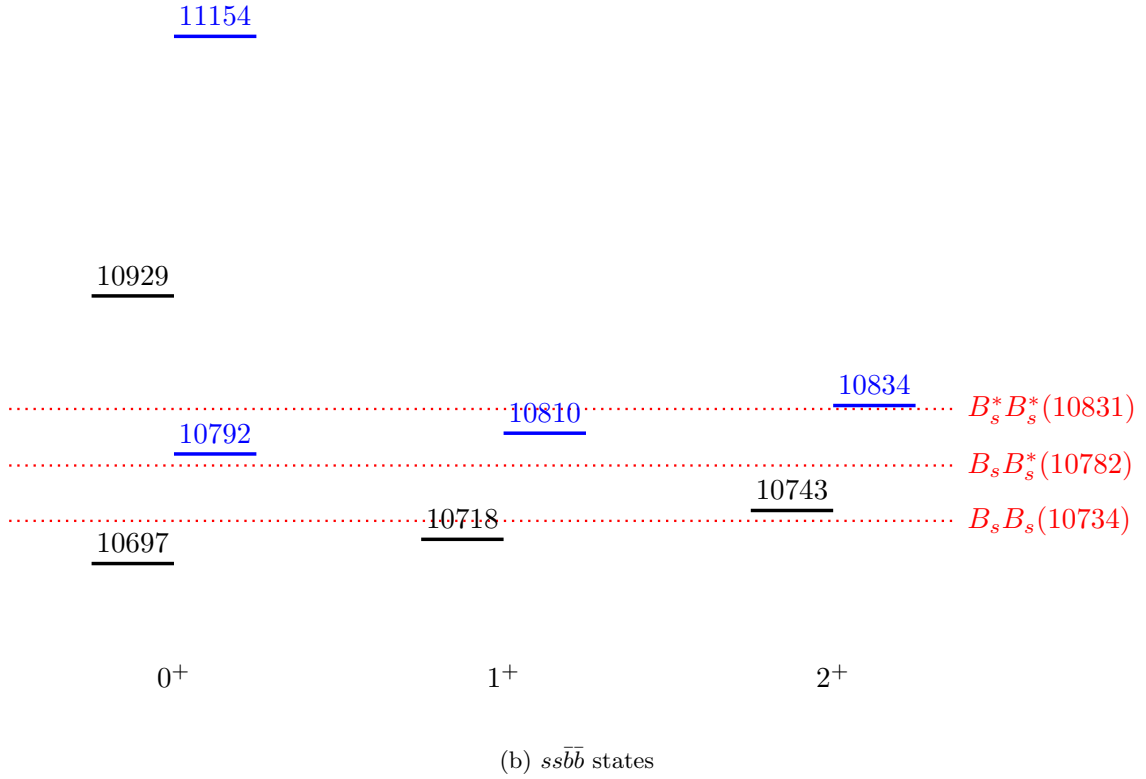
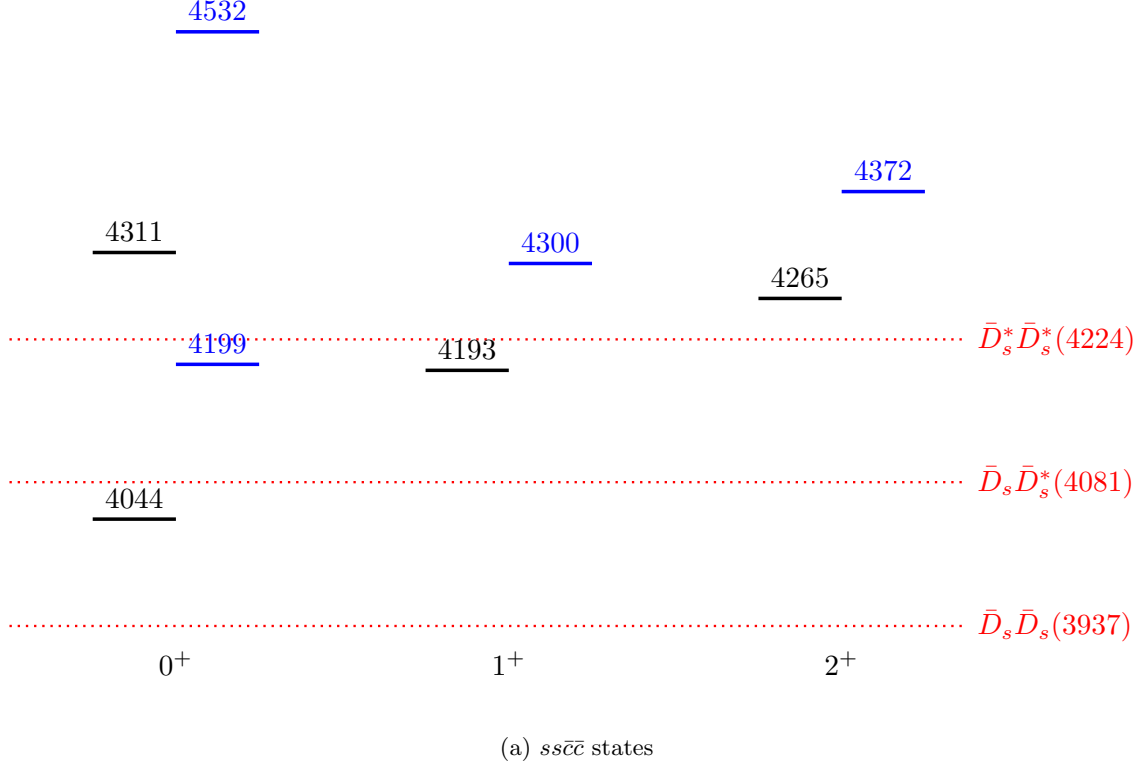


FIG. 3. Mass spectra of the $ss\bar{c}\bar{c}$ and $s\bar{s}b\bar{b}$ tetraquark states in scheme I (black) and scheme II (blue). The dotted lines indicate various meson-meson thresholds. The masses are all in units of MeV.

TABLE XIV. Masses and eigenvectors of the $ss\bar{c}\bar{c}$, $ss\bar{b}\bar{b}$ and $ss\bar{c}\bar{b}$ tetraquarks. The masses are all in units of MeV.

System	J^P	Scheme I		Scheme II	
		Mass	Eigenvector	Mass	Eigenvector
$ss\bar{c}\bar{c}$	0^+	4043.7	{0.650, 0.760}	4199.1	{0.442, 0.897}
		4311.1	{0.760, -0.650}	4532.1	{0.897, -0.442}
	1^+	4192.6	{1}	4300.2	{1}
	2^+	4264.5	{1}	4372.1	{1}
$ss\bar{b}\bar{b}$	0^+	10697.1	{0.196, 0.981}	10792.1	{0.124, 0.992}
		10928.8	{0.981, -0.196}	11154.3	{0.992, -0.124}
	1^+	10718.2	{1}	10809.8	{1}
	2^+	10742.5	{1}	10834.1	{1}
$ss\bar{c}\bar{b}$	0^+	7404.4	{0.547, 0.837}	7531.3	{0.325, 0.946}
		7597.3	{0.837, -0.547}	7818.8	{0.946, -0.325}
	1^+	7431.8	{-0.537, -0.551, 0.639}	7553.6	{-0.265, -0.662, 0.701}
		7503.3	{-0.096, 0.792, 0.603}	7603.5	{-0.047, 0.735, 0.677}
		7569.4	{0.838, -0.263, 0.478}	7795.3	{0.963, -0.146, 0.226}
	2^+	7534.3	{1}	7633.8	{1}

TABLE XV. The eigenvectors of the $ss\bar{c}\bar{c}$ tetraquark states in the $s\bar{c}\otimes s\bar{c}$ configuration. The masses are all in units of MeV.

System	J^P	Scheme I				Scheme II				
		Mass	$\bar{D}_s^*\bar{D}_s^*$	$\bar{D}_s^*\bar{D}_s$	$\bar{D}_s\bar{D}_s^*$	$\bar{D}_s\bar{D}_s$	Mass	$\bar{D}_s^*\bar{D}_s^*$	$\bar{D}_s^*\bar{D}_s$	$\bar{D}_s\bar{D}_s^*$
$ss\bar{c}\bar{c}$	0^+	4043.7	0.240		0.645	4199.1	0.054			0.629
		4311.1	0.725		-0.015	4532.1	0.762			0.145
	1^+	4192.6	0	0.408	0.408	4300.2	0	0.408	0.408	
	2^+	4264.5	0.577			4372.1	0.577			

TABLE XVI. The values of $k \cdot |c_i|^2$ for the $ss\bar{c}\bar{c}$ tetraquarks (in unit of MeV).

System	J^P	Scheme I			Scheme II		
		Mass	$\bar{D}_s^*\bar{D}_s^*$	$\bar{D}_s\bar{D}_s^*$	$\bar{D}_s\bar{D}_s$	Mass	$\bar{D}_s^*\bar{D}_s^*$
$ss\bar{c}\bar{c}$	0^+	4043.7	×	192.5	4199.1	×	289.1
		4311.1	226.4	0.2	4532.1	476.6	23.6
	1^+	4192.6		80.3	4300.2		113.0
	2^+	4264.5	97.5		4372.1	187.9	

TABLE XVII. The partial width ratios for the $ss\bar{c}\bar{c}$ tetraquarks. For each state, we choose one mode as the reference channel, and the partial width ratios of the other channels are calculated relative to this channel. The masses are all in unit of MeV.

System	J^P	Scheme I			Scheme II				
		Mass	$\bar{D}_s^*\bar{D}_s^*$	$\bar{D}_s\bar{D}_s^*$	$\bar{D}_s\bar{D}_s$	Mass	$\bar{D}_s^*\bar{D}_s^*$	$\bar{D}_s\bar{D}_s^*$	$\bar{D}_s\bar{D}_s$
$ss\bar{c}\bar{c}$	0^+	4043.7	×		1	4199.1	×		1
		4311.1	1185.7		1	4532.1	20.2		1
	1^+	4192.6		1		4300.2		1	
	2^+	4264.5	1			4372.1	1		

TABLE XVIII. The eigenvectors of the $ss\bar{b}\bar{b}$ tetraquark states in the $s\bar{b}\otimes s\bar{b}$ configuration. The masses are all in units of MeV.

System	J^P	Scheme I				Scheme II					
		Mass	$B_s^*B_s^*$	$B_s^*B_s$	$B_sB_s^*$	B_sB_s	Mass	$B_s^*B_s^*$	$B_s^*B_s$	$B_sB_s^*$	B_sB_s
$ss\bar{b}\bar{b}$	0^+	10697.1	-0.144			0.570	10792.1	-0.199			0.547
		10928.8	0.750			0.302	11154.3	0.737			0.343
	1^+	10718.2	0	0.408	0.408		10809.8	0	0.408	0.408	
	2^+	10742.5	0.577				10834.1	0.577			

TABLE XIX. The values of $k \cdot |c_i|^2$ for the $ss\bar{b}\bar{b}$ tetraquarks (in unit of MeV).

System	J^P	Scheme I				Scheme II			
		Mass	$B_s^*B_s^*$	$B_sB_s^*$	B_sB_s	Mass	$B_s^*B_s^*$	$B_sB_s^*$	B_sB_s
$ss\bar{b}\bar{b}$	0^+	10697.1	×		×	10792.1	×		167.6
		10928.8	410.8		93.8	11154.3	725.3		178.5
	1^+	10718.2		×		10809.8		64.3	
	2^+	10742.5	×			10834.1	44.4		

TABLE XX. The partial width ratios for the $ss\bar{b}\bar{b}$ tetraquarks. For each state, we choose one mode as the reference channel, and the partial width ratios of the other channels are calculated relative to this channel. The masses are all in unit of MeV.

System	J^P	Scheme I				Scheme II			
		Mass	$B_s^*B_s^*$	$B_sB_s^*$	B_sB_s	Mass	$B_s^*B_s^*$	$B_sB_s^*$	B_sB_s
$ss\bar{b}\bar{b}$	0^+	10697.1	×		×	10792.1	×		1
		10928.8	4.4		1	11154.3	4.1		1
	1^+	10718.2		×		10809.8		1	
	2^+	10742.5	×			10834.1	1		

IV. CONCLUSIONS

In this work, we systematically study the mass spectrum of the doubly heavy $qq\bar{Q}\bar{Q}$ tetraquarks in the frame-

work of an extended chromomagnetic model. In addition to the chromomagnetic interaction, the effect of color interaction is also considered in this model. The model pa-

TABLE XXI. The eigenvectors of the $ss\bar{c}\bar{b}$ tetraquark states in the $s\bar{c}\otimes s\bar{b}$ configuration. The masses are all in units of MeV.

System J^P	Scheme I				Scheme II				
	Mass	$\bar{D}_s^*B_s^*$	$\bar{D}_s^*B_s$	$\bar{D}_sB_s^*$	Mass	$\bar{D}_s^*B_s^*$	$\bar{D}_s^*B_s$	$\bar{D}_sB_s^*$	\bar{D}_sB_s
$ss\bar{c}\bar{b}$ 0^+	7404.4	0.145		0.642	7531.3	-0.043			0.606
	7597.3	0.750		0.068	7818.8	0.763			0.224
1^+	7431.8	-0.049	0.179	-0.629	7553.6	0.133	0.040	-0.581	
	7503.3	0.191	0.536	0.110	7603.5	0.249	0.515	0.085	
	7569.4	0.679	-0.311	0.097	7795.3	0.648	-0.388	0.268	
2^+	7534.3	0.577			7633.8	0.577			

TABLE XXII. The values of $k \cdot |c_i|^2$ for the $ss\bar{c}\bar{b}$ tetraquarks (in unit of MeV).

System J^P	Scheme I				Scheme II				
	Mass	$\bar{D}_s^*B_s^*$	$\bar{D}_s^*B_s$	$\bar{D}_sB_s^*$	Mass	$\bar{D}_s^*B_s^*$	$\bar{D}_s^*B_s$	$\bar{D}_sB_s^*$	\bar{D}_sB_s
$ss\bar{c}\bar{b}$ 0^+	7404.4	×		184.9	7531.3	0.2			279.4
	7597.3	260.2		4.1	7818.8	557.2			61.0
1^+	7431.8	×	×	147.8	7553.6	5.0	0.8	239.1	
	7503.3	×	78.3	7.2	7603.5	29.9	164.1	5.9	
	7569.4	165.0	51.1	6.9	7795.3	385.6	150.0	80.7	
2^+	7534.3	47.8			7633.8	190.8			

parameters are fitted from the mesons and baryons. Since the spatial configurations of the qq ($\bar{q}\bar{q}$) and $q\bar{q}$ pairs are different in the conventional hadrons and the tetraquarks, applying these parameters to the tetraquarks may cause errors. To appreciate this uncertainty, we adopt two schemes of parameters to study the $qq\bar{Q}\bar{Q}$ tetraquarks. As indicated in Eq. (41), the scheme II gives larger masses than the scheme I. However, the wave functions and decay properties of the two schemes are very similar for the $qq\bar{Q}\bar{Q}$ tetraquarks. We find three states which are stable in both schemes. They are the $nn\bar{b}\bar{b}$ tetraquark with quantum number $IJ^P = 01^+$, the $nn\bar{c}\bar{b}$ tetraquark with quantum number $IJ^P = 00^+$ and the $ns\bar{b}\bar{b}$ tetraquark with quantum number $J^P = 1^+$. They all lie below the thresholds of two pseudoscalar mesons, which can only decay through weak processes. Meanwhile, many narrow states which lie below S -wave decay channels are also found. It shall be interesting to search for these states.

The tetraquarks have two possible color configurations, namely the color-sextet configuration $|(qq)^{6_c}(\bar{Q}\bar{Q})^{6_c}\rangle$ and the color-triplet one $|(qq)^{3_c}(\bar{Q}\bar{Q})^{3_c}\rangle$. Unlike the fully heavy tetraquarks, the ground states of the doubly heavy tetraquarks favor the color-triplet configurations. Combining the results of fully and doubly heavy tetraquarks, we can clearly see the trend that the color-triplet config-

uration is more and more important when the mass ratio between the quarks and antiquarks increases.

Besides the mass spectrum, we also estimate the decay properties of the tetraquarks. We hope these states can be searched for by future experiments.

ACKNOWLEDGMENTS

X. Z. W. is grateful to Marek Karliner and Guang-Juan Wang for helpful comments and discussions. This project was supported by the National Natural Science Foundation of China (NSFC) under Grant No. 11975033 and No. 12070131001.

Appendix A: Wave function in the $q\bar{q}\otimes q\bar{q}$ configuration

To calculate the partial decay rates, we need to construct the tetraquark wave functions in the $q\bar{q}\otimes q\bar{q}$ configuration. The possible color-spin wave functions $\{\beta_i^J\}$ are listed as follows,

1. $J^P = 0^+$

$$\beta_1^0 = |(q_1\bar{q}_3)_1^8 (q_2\bar{q}_4)_1^8\rangle_0$$

TABLE XXIII. The partial width ratios for the $ss\bar{c}\bar{b}$ tetraquarks. For each state, we choose one mode as the reference channel, and the partial width ratios of the other channels are calculated relative to this channel. The masses are all in unit of MeV.

System J^P	Scheme I				Scheme II					
	Mass	$\bar{D}_s^* B_s^*$	$\bar{D}_s^* B_s$	$\bar{D}_s B_s^*$	$\bar{D}_s B_s$	Mass	$\bar{D}_s^* B_s^*$	$\bar{D}_s^* B_s$	$\bar{D}_s B_s^*$	$\bar{D}_s B_s$
$ss\bar{c}\bar{b}$ 0^+	7404.4	×			1	7531.3	0.0007			1
	7597.3	63.2			1	7818.8	9.1			1
1^+	7431.8	×	×	1		7553.6	0.02	0.003	1	
	7503.3	×	10.9	1		7603.5	5.1	27.8	1	
	7569.4	23.7	7.4	1		7795.3	4.8	1.9	1	
2^+	7534.3	1				7633.8	1			

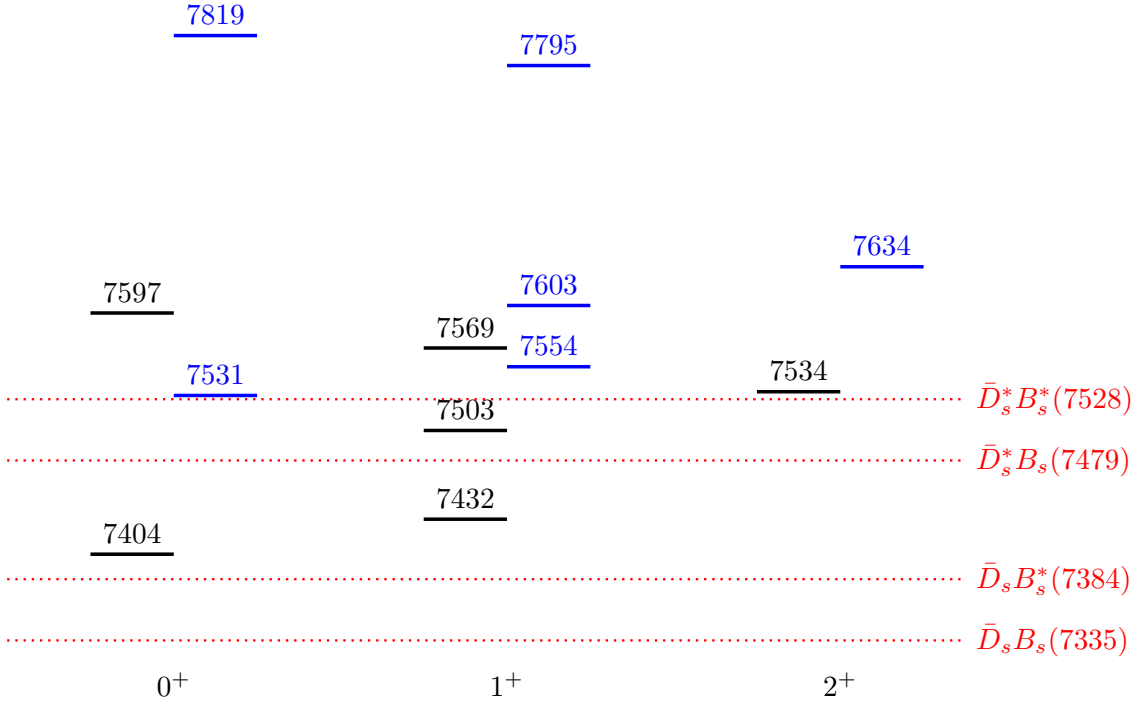


FIG. 4. Mass spectra of the $ss\bar{c}\bar{b}$ tetraquark states in scheme I (black) and scheme II (blue). The dotted lines indicate various meson-meson thresholds. The masses are all in units of MeV.

$$\begin{aligned}
\beta_2^0 &= |(q_1\bar{q}_3)_0^8 (q_2\bar{q}_4)_0^8\rangle_0 & \beta_5^1 &= |(q_1\bar{q}_3)_1^1 (q_2\bar{q}_4)_0^1\rangle_1 \\
\beta_3^0 &= |(q_1\bar{q}_3)_1^1 (q_2\bar{q}_4)_1^1\rangle_0 & \beta_6^1 &= |(q_1\bar{q}_3)_0^1 (q_2\bar{q}_4)_1^1\rangle_1 \\
\beta_3^0 &= |(q_1\bar{q}_3)_0^1 (q_2\bar{q}_4)_0^1\rangle_0 & &
\end{aligned} \tag{A1}$$

2. $J^P = 1^+$

$$\begin{aligned}
\beta_1^1 &= |(q_1\bar{q}_3)_1^8 (q_2\bar{q}_4)_1^8\rangle_1 & \beta_1^2 &= |(q_1\bar{q}_3)_1^8 (q_2\bar{q}_4)_1^8\rangle_2 \\
\beta_2^1 &= |(q_1\bar{q}_3)_1^8 (q_2\bar{q}_4)_0^8\rangle_1 & \beta_2^2 &= |(q_1\bar{q}_3)_1^1 (q_2\bar{q}_4)_1^1\rangle_2 \\
\beta_3^1 &= |(q_1\bar{q}_3)_0^8 (q_2\bar{q}_4)_1^8\rangle_1 & & \\
\beta_4^1 &= |(q_1\bar{q}_3)_1^1 (q_2\bar{q}_4)_1^1\rangle_1 & &
\end{aligned} \tag{A2}$$

3. $J^P = 2^+$

where the superscript 1 or 8 denotes the color, and the subscript 0, 1 or 2 denotes the spin. Among them, the

TABLE XXIV. Masses and eigenvectors of the $ns\bar{c}\bar{c}$, $ns\bar{b}\bar{b}$ and $ns\bar{c}\bar{b}$ tetraquarks. The masses are all in units of MeV.

System	J^P	Scheme I		Scheme II	
		Mass	Eigenvector	Mass	Eigenvector
$ns\bar{c}\bar{c}$	0^+	3937.6	{0.606, 0.795}	4085.7	{0.410, 0.912}
		4209.3	{0.795, -0.606}	4436.2	{0.912, -0.410}
	1^+	3919.0	{-0.534, -0.006, 0.845}	4051.5	{0.284, 0.005, -0.959}
		4073.0	{-0.032, -0.999, -0.027}	4180.2	{0.003, 0.99997, 0.007}
		4086.5	{0.845, -0.041, 0.534}	4328.9	{0.959, -0.005, 0.284}
	2^+	4144.3	{1}	4251.5	{1}
$ns\bar{b}\bar{b}$	0^+	10586.4	{0.163, 0.987}	10684.1	{0.107, 0.994}
		10854.6	{0.987, -0.163}	11090.2	{0.994, -0.107}
	1^+	10473.1	{0.082, 0.005, -0.997}	10569.0	{0.056, 0.005, -0.998}
		10605.3	{0.007, 0.99996, 0.006}	10700.5	{0.004, 0.99998, 0.005}
		10778.7	{0.997, -0.007, 0.082}	11016.1	{0.998, -0.004, 0.056}
	2^+	10628.7	{1}	10723.9	{1}
$ns\bar{c}\bar{b}$	0^+	7156.5	{0.647, 0.029, 0.038, 0.761}	7296.2	{0.375, 0.036, 0.050, 0.925}
		7299.0	{0.030, 0.473, 0.876, -0.087}	7421.1	{0.044, 0.283, 0.955, -0.080}
		7333.2	{-0.762, 0.070, 0.052, 0.642}	7547.8	{-0.926, 0.055, 0.058, 0.370}
		7506.6	{-0.023, -0.878, 0.477, 0.029}	7738.5	{-0.026, -0.957, 0.287, 0.032}
	1^+	7212.8	{0.423, -0.343, 0.031, 0.024, -0.025, 0.838}	7336.1	{0.181, -0.185, 0.035, 0.023, -0.030, 0.965}
		7323.9	{-0.210, 0.057, -0.413, -0.589, 0.635, 0.180}	7440.9	{-0.044, 0.030, -0.225, -0.675, 0.698, 0.060}
		7330.5	{-0.818, 0.168, 0.161, 0.095, -0.225, 0.466}	7487.8	{-0.089, -0.033, 0.041, -0.720, -0.687, 0.005}
		7386.1	{0.004, 0.224, -0.056, 0.749, 0.615, 0.089}	7565.3	{0.901, -0.351, -0.047, -0.090, -0.010, -0.233}
		7416.2	{0.329, 0.894, 0.062, -0.169, -0.144, 0.198}	7665.0	{-0.381, -0.916, -0.042, 0.039, 0.048, -0.102}
		7479.9	{0.013, -0.040, 0.892, -0.233, 0.383, -0.038}	7716.8	{-0.014, 0.042, -0.971, 0.129, -0.194, 0.037}
		2^+	7415.1	{0.297, 0.955}	7517.7
	7439.0		{0.955, -0.297}	7690.6	{0.998, -0.064}

TABLE XXV. The eigenvectors of the $ns\bar{c}\bar{c}$ tetraquark states in the $n\bar{c}\otimes s\bar{c}$ configuration. The masses are all in units of MeV.

System	J^P	Scheme I				Scheme II				
		Mass	$\bar{D}^*\bar{D}_s^*$	$\bar{D}^*\bar{D}_s$	$\bar{D}\bar{D}_s^*$	$\bar{D}\bar{D}_s$	Mass	$\bar{D}^*\bar{D}_s^*$	$\bar{D}^*\bar{D}_s$	$\bar{D}\bar{D}_s^*$
$ns\bar{c}\bar{c}$	0^+	3937.6	0.199		0.645	4085.7	0.026			0.623
		4209.3	0.737		0.022	4436.2	0.763			0.168
1^+		3919.0	0.036	-0.464	0.460	4051.5	-0.227	0.395	-0.391	
		4073.0	-0.029	-0.413	-0.403	4180.2	-0.005	-0.408	-0.409	
		4086.5	0.706	0.174	-0.207	4328.9	0.670	0.307	-0.311	
2^+		4144.3	0.577			4251.5	0.577			

TABLE XXVI. The values of $k \cdot |c_i|^2$ for the $ns\bar{c}\bar{c}$ tetraquarks (in unit of MeV).

System J^P	Scheme I				Scheme II					
	Mass	$\bar{D}^*\bar{D}_s^*$	$\bar{D}^*\bar{D}_s$	$\bar{D}\bar{D}_s^*$	$\bar{D}\bar{D}_s$	Mass	$\bar{D}^*\bar{D}_s^*$	$\bar{D}^*\bar{D}_s$	$\bar{D}\bar{D}_s^*$	$\bar{D}\bar{D}_s$
$ns\bar{c}\bar{c}$ 0^+	3937.6	×			185.3	4085.7	×			273.5
	4209.3	233.6			0.4	4436.2	478.6			31.3
1^+	3919.0	×	×	×	4051.5	×	60.4	58.0		
	4073.0	×	75.1	70.3	4180.2	0.008	107.1	106.8		
	4086.5	×	14.2	20.0	4328.9	297.3	80.7	82.5		
2^+	4144.3	73.7			4251.5	174.4				

TABLE XXVII. The partial width ratios for the $ns\bar{c}\bar{c}$ tetraquarks. For each state, we choose one mode as the reference channel, and the partial width ratios of the other channels are calculated relative to this channel. The masses are all in unit of MeV.

System J^P	Scheme I				Scheme II					
	Mass	$\bar{D}^*\bar{D}_s^*$	$\bar{D}^*\bar{D}_s$	$\bar{D}\bar{D}_s^*$	$\bar{D}\bar{D}_s$	Mass	$\bar{D}^*\bar{D}_s^*$	$\bar{D}^*\bar{D}_s$	$\bar{D}\bar{D}_s^*$	$\bar{D}\bar{D}_s$
$ns\bar{c}\bar{c}$ 0^+	3937.6	×			1	4085.7	×			1
	4209.3	569.1			1	4436.2	15.3			1
1^+	3919.0	×	×	×	4051.5	×	1.04	1		
	4073.0	×	1.1	1	4180.2	0.00007	1.003	1		
	4086.5	×	0.7	1	4328.9	3.6	0.98	1		
2^+	4144.3	1			4251.5	1				

TABLE XXVIII. The eigenvectors of the $ns\bar{b}\bar{b}$ tetraquark states in the $n\bar{b}\otimes s\bar{b}$ configuration. The masses are all in units of MeV.

System J^P	Scheme I				Scheme II					
	Mass	$B^*B_s^*$	B^*B_s	BB_s^*	BB_s	Mass	$B^*B_s^*$	B^*B_s	BB_s^*	BB_s
$ns\bar{b}\bar{b}$ 0^+	10586.4	-0.170			0.560	10684.1	-0.212			0.541
	10854.6	0.745			0.321	11090.2	0.734			0.353
1^+	10473.1	-0.360	0.323	-0.319		10569.0	-0.375	0.313	-0.309	
	10605.3	-0.006	-0.409	-0.407		10700.5	-0.004	-0.408	-0.408	
	10778.7	0.609	0.380	-0.386		11016.1	0.599	0.390	-0.393	
2^+	10628.7	0.577				10723.9	0.577			

TABLE XXIX. The values of $k \cdot |c_i|^2$ for the $ns\bar{b}\bar{b}$ tetraquarks (in unit of MeV).

System J^P	Scheme I					Scheme II				
	Mass	$B^*B_s^*$	B^*B_s	BB_s^*	BB_s	Mass	$B^*B_s^*$	B^*B_s	BB_s^*	BB_s
$ns\bar{b}\bar{b}$ 0^+	10586.4	×			×	10684.1	×			131.4
	10854.6	436.2			109.4	11090.2	744.5			193.1
1^+	10473.1	×	×	×		10569.0	×	×	×	
	10605.3	×	×	×		10700.5	×	36.6	28.9	
	10778.7	168.9	99.0	100.0		11016.1	439.9	201.8	204.1	
2^+	10628.7	×				10723.9	×			

TABLE XXX. The partial width ratios for the $ns\bar{b}\bar{b}$ tetraquarks. For each state, we choose one mode as the reference channel, and the partial width ratios of the other channels are calculated relative to this channel. The masses are all in unit of MeV.

System J^P	Scheme I					Scheme II				
	Mass	$B^*B_s^*$	B^*B_s	BB_s^*	BB_s	Mass	$B^*B_s^*$	B^*B_s	BB_s^*	BB_s
$ns\bar{b}\bar{b}$ 0^+	10586.4	×			×	10684.1	×			1
	10854.6	4.0			1	11090.2	3.9			1
1^+	10473.1	×	×	×		10569.0	×	×	×	
	10605.3	×	×	×		10700.5	×	1.3	1	
	10778.7	1.7	1.0	1		11016.1	2.2	1.0	1	
2^+	10628.7	×				10723.9	×			

TABLE XXXI. The eigenvectors of the $ns\bar{c}\bar{b}$ tetraquark states in the $n\bar{c}\otimes s\bar{b}$ configuration. The masses are all in units of MeV.

System J^P	Scheme I					Scheme II				
	Mass	$\bar{D}^*B_s^*$	\bar{D}^*B_s	$\bar{D}B_s^*$	$\bar{D}B_s$	Mass	$\bar{D}^*B_s^*$	\bar{D}^*B_s	$\bar{D}B_s^*$	$\bar{D}B_s$
$ns\bar{c}\bar{b}$ 0^+	7156.5	0.126			0.708	7296.2	-0.320			-0.572
	7299.0	-0.026			-0.627	7421.1	0.134			-0.601
	7333.2	-0.666			0.299	7547.8	-0.585			0.496
	7506.6	-0.735			-0.128	7738.5	-0.733			-0.256
1^+	7212.8	0.152	-0.148	0.655		7336.1	0.295	-0.263	0.491	
	7323.9	0.127	-0.039	-0.685		7440.9	0.197	-0.012	-0.589	
	7330.5	0.289	-0.630	-0.237		7487.8	-0.273	-0.575	-0.115	
	7386.1	0.384	0.574	0.042		7565.3	-0.329	0.424	0.544	
	7416.2	0.574	0.362	-0.120		7665.0	-0.575	-0.517	0.109	
	7479.9	0.633	-0.346	0.171		7716.8	-0.600	0.391	-0.302	
2^+	7415.1	0.794				7517.7	0.629			
	7439.0	0.608				7690.6	0.778			

TABLE XXXII. The eigenvectors of the $ns\bar{c}\bar{b}$ tetraquark states in the $n\bar{b}\otimes s\bar{c}$ configuration. The masses are all in units of MeV.

System	J^P	Scheme I				Scheme II					
		Mass	$B^*\bar{D}_s^*$	$B^*\bar{D}_s$	$B\bar{D}_s^*$	$B\bar{D}_s$	Mass	$B^*\bar{D}_s^*$	$B^*\bar{D}_s$	$B\bar{D}_s^*$	$B\bar{D}_s$
$ns\bar{c}\bar{b}$	0^+	7156.5	0.107		0.646	7296.2	-0.298				-0.493
		7299.0	0.137		0.635	7421.1	-0.018				0.584
		7333.2	-0.598		0.407	7547.8	-0.541				0.599
		7506.6	0.783		0.112	7738.5	0.786				0.238
1^+		7212.8	-0.136	0.596	-0.128	7336.1	-0.279	0.426	-0.236		
		7323.9	-0.086	0.500	-0.261	7440.9	0.114	0.549	-0.048		
		7330.5	-0.286	-0.576	-0.447	7487.8	-0.240	0.042	0.443		
		7386.1	0.054	-0.169	-0.438	7565.3	0.266	0.649	0.465		
		7416.2	-0.621	-0.116	0.634	7665.0	0.566	0.140	-0.612		
		7479.9	0.710	-0.146	0.351	7716.8	-0.679	0.273	-0.395		
2^+		7415.1	-0.308			7517.7	-0.524				
		7439.0	0.951			7690.6	0.852				

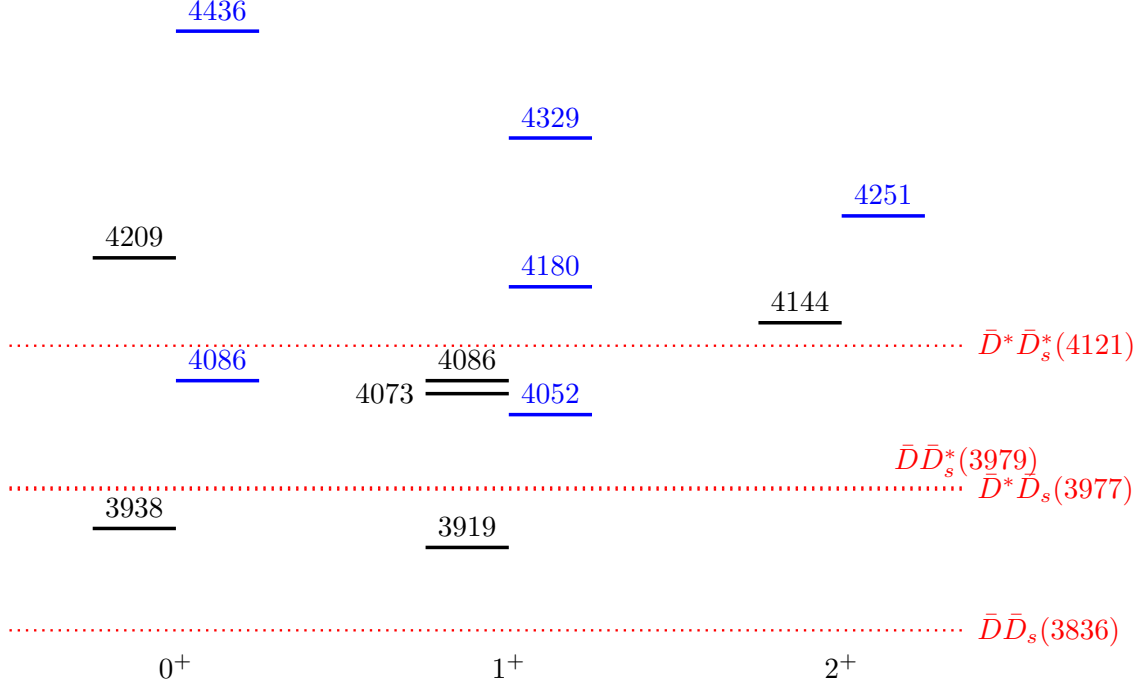
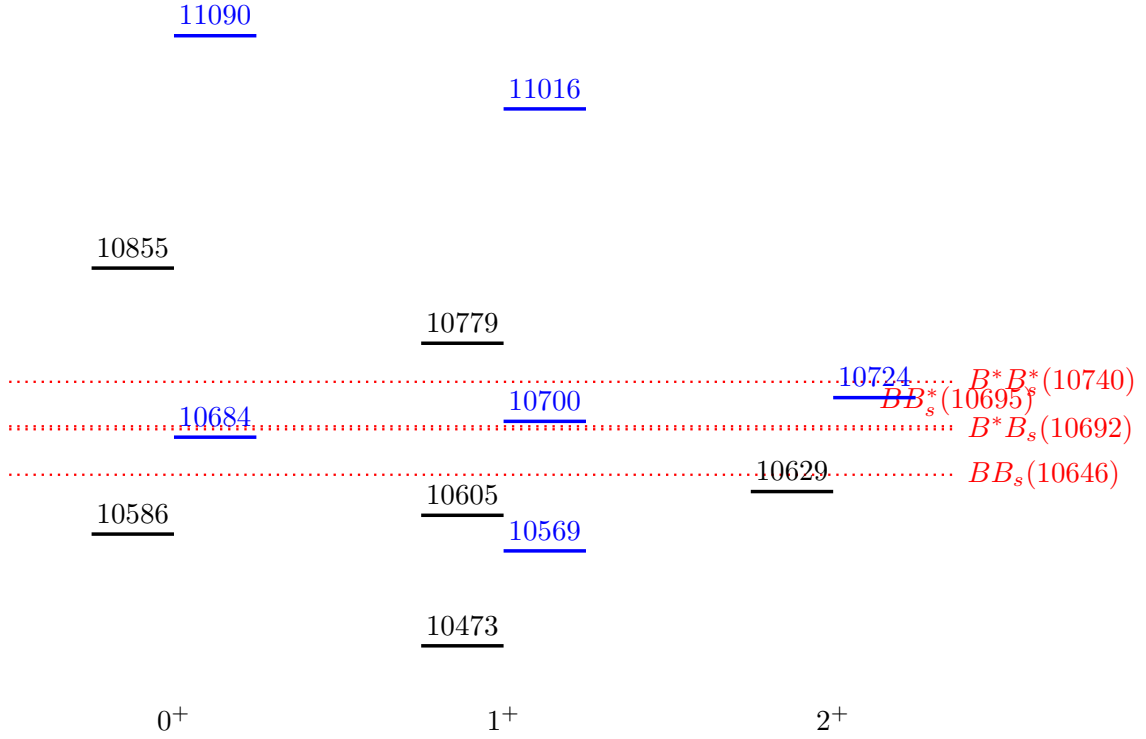
(a) $ns\bar{c}c$ states(b) $ns\bar{b}b$ states

FIG. 5. Mass spectra of the $ns\bar{c}c$ and $ns\bar{b}b$ tetraquark states in scheme I (black) and scheme II (blue). The dotted lines indicate various meson-meson thresholds. The masses are all in units of MeV.

TABLE XXXIII. The values of $k \cdot |c_i|^2$ for the $ns\bar{c}\bar{b}$ tetraquarks (in unit of MeV).

System	J^P	Scheme I				Scheme II					
		Mass	$\bar{D}^*B_s^*$	\bar{D}^*B_s	$\bar{D}B_s^*$	$\bar{D}B_s$	Mass	$\bar{D}^*B_s^*$	\bar{D}^*B_s	$\bar{D}B_s^*$	$\bar{D}B_s$
$ns\bar{c}\bar{b}$	0^+	7156.5	×			×	7296.2	×			136.2
		7299.0	×			167.7	7421.1	×			263.8
		7333.2	×			47.1	7547.8	207.8			234.9
		7506.6	267.1			14.5	7738.5	527.0			80.5
	1^+	7212.8	×	×	×		7336.1	×	×		93.3
		7323.9	×	×	159.4		7440.9	8.7	0.07		232.6
		7330.5	×	×	20.6		7487.8	32.4	190.9		10.2
		7386.1	×	58.5	1.0		7565.3	70.5	135.6		267.3
		7416.2	×	45.3	8.9		7665.0	282.4	250.9		12.7
		7479.9	162.8	66.8	22.0		7716.8	340.3	156.4		103.6
	2^+	7415.1	×				7517.7	208.5			
		7439.0	77.7				7690.6	544.2			

System	J^P	Scheme I				Scheme II					
		Mass	$B^*\bar{D}_s^*$	$B^*\bar{D}_s$	$B\bar{D}_s^*$	$B\bar{D}_s$	Mass	$B^*\bar{D}_s^*$	$B^*\bar{D}_s$	$B\bar{D}_s^*$	$B\bar{D}_s$
$ns\bar{c}\bar{b}$	0^+	7156.5	×			×	7296.2	×			90.9
		7299.0	×			155.3	7421.1	×			243.7
		7333.2	×			82.7	7547.8	170.9			339.5
		7506.6	282.8			11.0	7738.5	601.5			69.5
	1^+	7212.8	×	×	×		7336.1	×	64.1	×	
		7323.9	×	74.7	×		7440.9	1.4	198.4	0.9	
		7330.5	×	109.2	×		7487.8	22.6	1.4		106.4
		7386.1	×	14.8	×		7565.3	44.6	379.9		158.0
		7416.2	×	8.0	109.6		7665.0	269.8	20.7		345.5
		7479.9	182.6	15.8	63.8		7716.8	431.6	84.8		157.8
	2^+	7415.1	×				7517.7	136.4			
		7439.0	75.0				7690.6	646.2			

TABLE XXXIV. The partial width ratios for the $ns\bar{c}\bar{b}$ tetraquarks. For each state, we choose one mode as the reference channel, and the partial width ratios of the other channels are calculated relative to this channel. The masses are all in unit of MeV.

System J^P	Scheme I				Scheme II					
	Mass	$\bar{D}^*B_s^*$	\bar{D}^*B_s	$\bar{D}B_s^*$	$\bar{D}B_s$	Mass	$\bar{D}^*B_s^*$	\bar{D}^*B_s	$\bar{D}B_s^*$	$\bar{D}B_s$
$ns\bar{c}\bar{b}$ 0^+	7156.5	×			×	7296.2	×			1
	7299.0	×			1	7421.1	×			1
	7333.2	×			1	7547.8	0.9			1
	7506.6	18.4			1	7738.5	6.6			1
	7212.8	×	×	×		7336.1	×	×		1
	7323.9	×	×	1		7440.9	0.04	0.0003		1
	7330.5	×	×	1		7487.8	3.2	18.8		1
	7386.1	×	61.5	1		7565.3	0.3	0.5		1
	7416.2	×	5.1	1		7665.0	22.3	19.8		1
	7479.9	7.4	3.0	1		7716.8	3.3	1.5		1
2^+	7415.1	×				7517.7	1			
	7439.0	1				7690.6	1			

System J^P	Scheme I				Scheme II					
	Mass	$B^*\bar{D}_s^*$	$B^*\bar{D}_s$	$B\bar{D}_s^*$	$B\bar{D}_s$	Mass	$B^*\bar{D}_s^*$	$B^*\bar{D}_s$	$B\bar{D}_s^*$	$B\bar{D}_s$
$ns\bar{c}\bar{b}$ 0^+	7156.5	×			×	7296.2	×			1
	7299.0	×			1	7421.1	×			1
	7333.2	×			1	7547.8	0.5			1
	7506.6	25.8			1	7738.5	8.7			1
	7212.8	×	×	×		7336.1	×	1	×	
	7323.9	×	1	×		7440.9	0.007	1	0.005	
	7330.5	×	1	×		7487.8	16.7	1	78.4	
	7386.1	×	1	×		7565.3	0.1	1	0.4	
	7416.2	×	1	13.6		7665.0	13.0	1	16.7	
	7479.9	11.5	1	4.0		7716.8	5.1	1	1.9	
2^+	7415.1	×				7517.7	1			
	7439.0	1				7690.6	1			

$1_c \otimes 1_c$ bases can also be written as combinations of two mesons. For example, $|(n_1\bar{c}_3)_1^1(n_2\bar{c}_4)_1^1\rangle_J \equiv |\bar{D}^*\bar{D}^*\rangle_J$.

- [1] Y. Cui, X.-L. Chen, W.-Z. Deng, and S.-L. Zhu, Possible Heavy Tetraquarks $qQ\bar{q}\bar{Q}$, $qq\bar{Q}\bar{Q}$ and $qQ\bar{Q}\bar{Q}$, *HEP NP* **31**, 7 (2007), [arXiv:hep-ph/0607226](#) [hep-ph].
- [2] W. Park and S. H. Lee, Color spin wave functions of heavy tetraquark states, *Nucl. Phys.* **A925**, 161 (2014), [arXiv:1311.5330](#) [nucl-th].
- [3] J.-J. Wu, R. Molina, E. Oset, and B. S. Zou, Prediction of Narrow N^* and Λ^* Resonances with Hidden Charm above 4 GeV, *Phys. Rev. Lett.* **105**, 232001 (2010), [arXiv:1007.0573](#) [nucl-th].
- [4] X.-H. Liu, Q. Wang, and Q. Zhao, Understanding the newly observed heavy pentaquark candidates, *Phys. Lett.* **B757**, 231 (2016), [arXiv:1507.05359](#) [hep-ph].
- [5] E. S. Swanson, Short range structure in the $X(3872)$, *Phys. Lett.* **B588**, 189 (2004), [arXiv:hep-ph/0311229](#) [hep-ph].

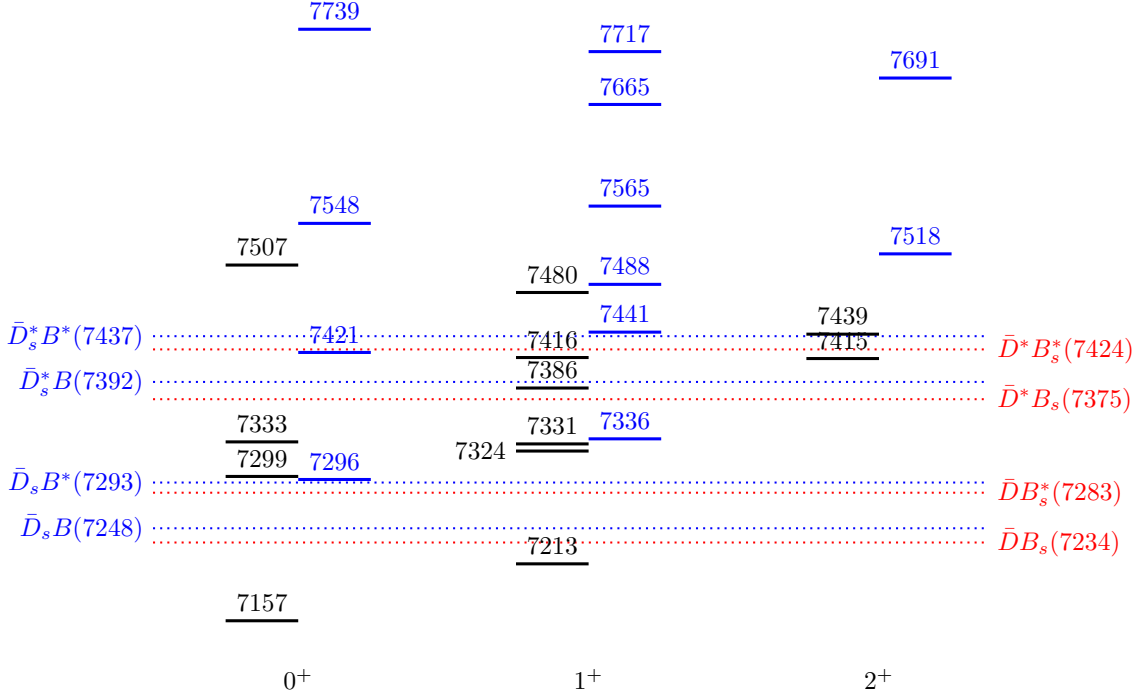


FIG. 6. Mass spectra of the $ns\bar{c}\bar{b}$ tetraquark states in scheme I (black) and scheme II (blue). The dotted lines indicate various meson-meson thresholds. The masses are all in units of MeV.

- [6] T. F. Caramés, A. Valcarce, and J. Vijande, Charged charmonium molecules, *Phys. Rev.* **D82**, 054032 (2010).
- [7] R. Chen, X. Liu, Y.-R. Liu, and S.-L. Zhu, Predictions of the hidden-charm molecular states with the four quark components, *Eur. Phys. J.* **C76**, 319 (2016), [arXiv:1511.03439 \[hep-ph\]](#).
- [8] C. E. Carlson, T. H. Hansson, and C. Peterson, Meson, Baryon and Glueball Masses in the MIT Bag Model, *Phys. Rev.* **D27**, 1556 (1983).
- [9] H.-X. Chen, W. Chen, and S.-L. Zhu, Toward the existence of the odderon as a three-gluon bound state, *Phys. Rev. D* **103**, L091503 (2021), [arXiv:2103.17201 \[hep-ph\]](#).
- [10] S.-L. Zhu, The possible interpretations of $Y(4260)$, *Phys. Lett.* **B625**, 212 (2005), [arXiv:hep-ph/0507025 \[hep-ph\]](#).
- [11] A. Esposito, A. Pilloni, and A. D. Polosa, Hybridized Tetraquarks, *Phys. Lett.* **B758**, 292 (2016), [arXiv:1603.07667 \[hep-ph\]](#).
- [12] S. K. Choi *et al.* (Belle Collaboration), Observation of a Narrow Charmoniumlike State in Exclusive $B^\pm \rightarrow K^\pm \pi^+ \pi^- J/\psi$ Decays, *Phys. Rev. Lett.* **91**, 262001 (2003), [arXiv:hep-ex/0309032 \[hep-ex\]](#).
- [13] P. A. Zyla *et al.* (Particle Data Group), Review of Particle Physics, *PTEP* **2020**, 083C01 (2020).
- [14] B. Aubert *et al.* (BaBar Collaboration), Observation of a Broad Structure in the $\pi^+ \pi^- J/\psi$ Mass Spectrum around 4.26 GeV/ c^2 , *Phys. Rev. Lett.* **95**, 142001 (2005), [arXiv:hep-ex/0506081 \[hep-ex\]](#).
- [15] M. Ablikim *et al.* (BESIII Collaboration), Observation of a Charged Charmoniumlike Structure in $e^+ e^- \rightarrow \pi^+ \pi^- J/\psi$ at $\sqrt{s}=4.26$ GeV, *Phys. Rev. Lett.* **110**, 252001 (2013), [arXiv:1303.5949 \[hep-ex\]](#).
- [16] Z. Q. Liu *et al.* (Belle Collaboration), Study of $e^+ e^- \rightarrow \pi^+ \pi^- J/\psi$ and Observation of a Charged Charmoniumlike State at Belle, *Phys. Rev. Lett.* **110**, 252002 (2013), [Erratum: *Phys. Rev. Lett.* 111, 019901 (2013)], [arXiv:1304.0121 \[hep-ex\]](#).
- [17] A. Bondar *et al.* (Belle Collaboration), Observation of Two Charged Bottomoniumlike Resonances in $\Upsilon(5S)$ Decays, *Phys. Rev. Lett.* **108**, 122001 (2012), [arXiv:1110.2251 \[hep-ex\]](#).
- [18] R. Aaij *et al.* (LHCb Collaboration), Observation of structure in the J/ψ -pair mass spectrum, *Sci. Bull.* **65**, 1983 (2020), [arXiv:2006.16957 \[hep-ex\]](#).
- [19] H.-X. Chen, W. Chen, X. Liu, and S.-L. Zhu, The hidden-charm pentaquark and tetraquark states, *Phys. Rept.* **639**, 1 (2016), [arXiv:1601.02092 \[hep-ph\]](#).
- [20] A. Esposito, A. Pilloni, and A. D. Polosa, Multiquark Resonances, *Phys. Rept.* **668**, 1 (2017), [arXiv:1611.07920 \[hep-ph\]](#).
- [21] R. F. Lebed, R. E. Mitchell, and E. S. Swanson, Heavy-quark QCD exotica, *Prog. Part. Nucl. Phys.* **93**, 143 (2017), [arXiv:1610.04528 \[hep-ph\]](#).
- [22] A. Ali, J. S. Lange, and S. Stone, Exotics: Heavy pentaquarks and tetraquarks, *Prog. Part. Nucl. Phys.* **97**, 123 (2017), [arXiv:1706.00610 \[hep-ph\]](#).
- [23] F.-K. Guo, C. Hanhart, U.-G. Meißner, Q. Wang, Q. Zhao, and B.-S. Zou, Hadronic molecules, *Rev. Mod. Phys.* **90**, 015004 (2018), [arXiv:1705.00141 \[hep-ph\]](#).
- [24] C.-Z. Yuan, The XYZ states revisited, *Int. J. Mod. Phys.* **A33**, 1830018 (2018), [arXiv:1808.01570 \[hep-ex\]](#).

- [25] N. Brambilla, S. Eidelman, C. Hanhart, A. Nefediev, C.-P. Shen, C. E. Thomas, A. Vairo, and C.-Z. Yuan, The XYZ states: Experimental and theoretical status and perspectives, *Phys. Rept.* **873**, 1 (2020), [arXiv:1907.07583 \[hep-ex\]](#).
- [26] Y.-R. Liu, H.-X. Chen, W. Chen, X. Liu, and S.-L. Zhu, Pentaquark and Tetraquark States, *Prog. Part. Nucl. Phys.* **107**, 237 (2019), [arXiv:1903.11976 \[hep-ph\]](#).
- [27] R. Aaij *et al.* (LHCb Collaboration), Observation of the Doubly Charmed Baryon Ξ_{cc}^{++} , *Phys. Rev. Lett.* **119**, 112001 (2017), [arXiv:1707.01621 \[hep-ex\]](#).
- [28] E. J. Eichten and C. Quigg, Heavy-Quark Symmetry Implies Stable Heavy Tetraquark Mesons $Q_i Q_j \bar{q}_k \bar{q}_l$, *Phys. Rev. Lett.* **119**, 202002 (2017), [arXiv:1707.09575 \[hep-ph\]](#).
- [29] M. Karliner and J. L. Rosner, Discovery of the Doubly Charmed Ξ_{cc} Baryon Implies a Stable $bb\bar{u}\bar{d}$ Tetraquark, *Phys. Rev. Lett.* **119**, 202001 (2017), [arXiv:1707.07666 \[hep-ph\]](#).
- [30] R. Aaij *et al.* (LHCb Collaboration), Observation of an exotic narrow doubly charmed tetraquark, (2021), [arXiv:2109.01038 \[hep-ex\]](#).
- [31] R. Aaij *et al.* (LHCb Collaboration), Study of the doubly charmed tetraquark T_{cc}^+ , (2021), [arXiv:2109.01056 \[hep-ex\]](#).
- [32] F. Muheim (LHCb Collaboration), Highlights from the LHCb experiment, in *European Physical Society Conference on High Energy Physics (EPS-HEP) 2021* (2021).
- [33] I. Polyakov (LHCb Collaboration), Recent LHCb results on exotic meson candidates, in *European Physical Society Conference on High Energy Physics (EPS-HEP) 2021* (2021).
- [34] N. Li, Z.-F. Sun, X. Liu, and S.-L. Zhu, Coupled-channel analysis of the possible $D^{(*)}D^{(*)}$, $\bar{B}^{(*)}\bar{B}^{(*)}$ and $D^{(*)}\bar{B}^{(*)}$ molecular states, *Phys. Rev. D* **88**, 114008 (2013), [arXiv:1211.5007 \[hep-ph\]](#).
- [35] S. S. Agaev, K. Azizi, and H. Sundu, Newly observed exotic doubly charmed meson T_{cc}^+ , (2021), [arXiv:2108.00188 \[hep-ph\]](#).
- [36] R. Chen, Q. Huang, X. Liu, and S.-L. Zhu, Another doubly charmed molecular resonance $T_{cc}^+(3876)$, (2021), [arXiv:2108.01911 \[hep-ph\]](#).
- [37] L.-Y. Dai, X. Sun, X.-W. Kang, A. P. Szczepaniak, and J.-S. Yu, Pole analysis on the doubly charmed meson in $D^0 D^0 \pi^+$ mass spectrum, (2021), [arXiv:2108.06002 \[hep-ph\]](#).
- [38] X.-K. Dong, F.-K. Guo, and B.-S. Zou, A survey of heavy-heavy hadronic molecules, (2021), [arXiv:2108.02673 \[hep-ph\]](#).
- [39] A. Feijoo, W. t. Liang, and E. Oset, $D^0 D^0 \pi^+$ mass distribution in the production of the T_{cc} exotic state, (2021), [arXiv:2108.02730 \[hep-ph\]](#).
- [40] X.-Z. Ling, M.-Z. Liu, L.-S. Geng, E. Wang, and J.-J. Xie, Can we understand the decay width of the T_{cc}^+ state?, (2021), [arXiv:2108.00947 \[hep-ph\]](#).
- [41] N. Li, Z.-F. Sun, X. Liu, and S.-L. Zhu, Perfect DD^* molecular prediction matching the T_{cc} observation at LHCb, (2021), [arXiv:2107.13748 \[hep-ph\]](#).
- [42] L. Meng, G.-J. Wang, B. Wang, and S.-L. Zhu, Strong and electromagnetic decays in the long-distance to identify the structure of the T_{cc}^+ , (2021), [arXiv:2107.14784 \[hep-ph\]](#).
- [43] T.-W. Wu, Y.-W. Pan, M.-Z. Liu, S.-Q. Luo, X. Liu, and L.-S. Geng, Discovery of the doubly charmed T_{cc}^+ state implies a triply charmed H_{ccc} hexaquark state, (2021), [arXiv:2108.00923 \[hep-ph\]](#).
- [44] M.-J. Yan and M. P. Valderrama, Two-body operators and the decay width of the T_{cc}^+ tetraquark, (2021), [arXiv:2108.04785 \[hep-ph\]](#).
- [45] J. P. Ader, J. M. Richard, and P. Taxil, Do narrow heavy multi-quark states exist?, *Phys. Rev.* **D25**, 2370 (1982).
- [46] J. Carlson, L. Heller, and J. A. Tjon, Stability of dimesons, *Phys. Rev.* **D37**, 744 (1988).
- [47] S. Zouzou, B. Silvestre-Brac, C. Gignoux, and J. M. Richard, Four-Quark Bound States, *Z. Phys.* **C30**, 457 (1986).
- [48] B. Silvestre-Brac and C. Semay, Systematics of $L = 0$ $q^2 \bar{q}^2$ systems, *Z. Phys.* **C57**, 273 (1993).
- [49] B. A. Gelman and S. Nussinov, Does a narrow tetraquark $cc\bar{u}\bar{d}$ state exist?, *Phys. Lett.* **B551**, 296 (2003), [arXiv:hep-ph/0209095 \[hep-ph\]](#).
- [50] J. Vijande, F. Fernandez, A. Valcarce, and B. Silvestre-Brac, Tetraquarks in a chiral constituent quark model, *Eur. Phys. J.* **A19**, 383 (2004), [arXiv:hep-ph/0310007 \[hep-ph\]](#).
- [51] D. Janc and M. Rosina, The $T_{cc} = DD^*$ Molecular State, *Few Body Syst.* **35**, 175 (2004), [arXiv:hep-ph/0405208](#).
- [52] J. Vijande, A. Valcarce, and K. Tsushima, Dynamical study of $QQ - \bar{u}\bar{d}$ mesons, *Phys. Rev.* **D74**, 054018 (2006), [arXiv:hep-ph/0608316 \[hep-ph\]](#).
- [53] J. Vijande, A. Valcarce, and J. M. Richard, Stability of multi-quarks in a simple string model, *Phys. Rev.* **D76**, 114013 (2007), [arXiv:0707.3996 \[hep-ph\]](#).
- [54] D. Ebert, R. N. Faustov, V. O. Galkin, and W. Lucha, Masses of tetraquarks with two heavy quarks in the relativistic quark model, *Phys. Rev.* **D76**, 114015 (2007), [arXiv:0706.3853 \[hep-ph\]](#).
- [55] S. H. Lee and S. Yasui, Stable multi-quark states with heavy quarks in a diquark model, *Eur. Phys. J.* **C64**, 283 (2009), [arXiv:0901.2977 \[hep-ph\]](#).
- [56] Y. Yang, C. Deng, J. Ping, and T. Goldman, S -wave $QQ\bar{q}\bar{q}$ state in the constituent quark model, *Phys. Rev.* **D80**, 114023 (2009).
- [57] A. Valcarce, J. Vijande, and T. F. Caramés, Doubly Charmed Mesons, *Proceedings, 4th International Workshop on Charm Physics (Charm 2010): Beijing, China, October 21-24, 2010*, *Int. J. Mod. Phys. Conf. Ser.* **2**, 173 (2011), [arXiv:1012.4627 \[hep-ph\]](#).
- [58] S.-Q. Luo, K. Chen, X. Liu, Y.-R. Liu, and S.-L. Zhu, Exotic tetraquark states with the $qq\bar{Q}\bar{Q}$ configuration, *Eur. Phys. J.* **C77**, 709 (2017), [arXiv:1707.01180 \[hep-ph\]](#).
- [59] C. Deng, H. Chen, and J. Ping, Systematical investigation on the stability of doubly heavy tetraquark states, *Eur. Phys. J.* **A 56**, 9 (2020), [arXiv:1811.06462 \[hep-ph\]](#).
- [60] W. Park, S. Noh, and S. H. Lee, Masses of the doubly heavy tetraquarks in a constituent quark model, *Nucl. Phys.* **A983**, 1 (2019), [arXiv:1809.05257 \[nucl-th\]](#).
- [61] X. Yan, B. Zhong, and R. Zhu, Doubly charmed tetraquarks in a diquark-antidiquark model, *Int. J. Mod. Phys.* **A33**, 1850096 (2018), [arXiv:1804.06761 \[hep-ph\]](#).
- [62] L. Maiani, A. D. Polosa, and V. Riquer, Hydrogen bond of QCD in doubly heavy baryons and tetraquarks, *Phys. Rev.* **D100**, 074002 (2019), [arXiv:1908.03244 \[hep-ph\]](#).

- [63] G. Yang, J. Ping, and J. Segovia, Doubly-heavy tetraquarks, *Phys. Rev. D* **101**, 014001 (2020), [arXiv:1911.00215 \[hep-ph\]](#).
- [64] R. Zhu, X. Liu, H. Huang, and C.-F. Qiao, Analyzing doubly heavy tetra- and penta-quark states by variational method, *Phys. Lett. B* **797**, 134869 (2019), [arXiv:1904.10285 \[hep-ph\]](#).
- [65] E. Braaten, L.-P. He, and A. Mohapatra, Masses of doubly heavy tetraquarks with error bars, *Phys. Rev. D* **103**, 016001 (2021), [arXiv:2006.08650 \[hep-ph\]](#).
- [66] J.-B. Cheng, S.-Y. Li, Y.-R. Liu, Z.-G. Si, and T. Yao, Double-heavy tetraquark states with heavy diquark-antiquark symmetry, *Chin. Phys. C* **45**, 043102 (2021), [arXiv:2008.00737 \[hep-ph\]](#).
- [67] Q.-F. Lü, D.-Y. Chen, and Y.-B. Dong, Masses of doubly heavy tetraquarks $T_{QQ'}$ in a relativized quark model, *Phys. Rev. D* **102**, 034012 (2020), [arXiv:2006.08087 \[hep-ph\]](#).
- [68] Q. Meng, E. Hiyama, A. Hosaka, M. Oka, P. Gubler, K. U. Can, T. T. Takahashi, and H. S. Zong, Stable double-heavy tetraquarks: Spectrum and structure, *Phys. Lett. B* **814**, 136095 (2021), [arXiv:2009.14493 \[nucl-th\]](#).
- [69] Y. Tan, W. Lu, and J. Ping, Systematics of $QQ\bar{q}\bar{q}$ in a chiral constituent quark model, *Eur. Phys. J. Plus* **135**, 716 (2020), [arXiv:2004.02106 \[hep-ph\]](#).
- [70] R. N. Faustov, V. O. Galkin, and E. M. Savchenko, Heavy Tetraquarks in the Relativistic Quark Model, *Universe* **7**, 94 (2021), [arXiv:2103.01763 \[hep-ph\]](#).
- [71] Q. Meng, M. Harada, E. Hiyama, A. Hosaka, and M. Oka, Doubly Heavy Tetraquark Resonant States, (2021), [arXiv:2106.11868 \[hep-ph\]](#).
- [72] S. Noh, W. Park, and S. H. Lee, Doubly heavy tetraquarks, $qq'QQ'$, in a nonrelativistic quark model with a complete set of harmonic oscillator bases [10.1103/PhysRevD.103.114009](#) (2021), [arXiv:2102.09614 \[hep-ph\]](#).
- [73] F. S. Navarra, M. Nielsen, and S. H. Lee, QCD sum rules study of $QQ - \bar{u}\bar{d}$ mesons, *Phys. Lett. B* **649**, 166 (2007), [arXiv:hep-ph/0703071](#).
- [74] Z.-G. Wang, Y.-M. Xu, and H.-J. Wang, Analysis of Scalar Doubly Heavy Tetraquark States with QCD Sum Rules, *Commun. Theor. Phys.* **55**, 1049 (2011), [arXiv:1004.0484 \[hep-ph\]](#).
- [75] J. M. Dias, S. Narison, F. S. Navarra, M. Nielsen, J. M. Richard, S. Narison, and J. M. Richard, Relation between $T_{cc,bb}$ and $X_{c,b}$ from QCD, *Phys. Lett. B* **703**, 274 (2011), [arXiv:1105.5630 \[hep-ph\]](#).
- [76] M.-L. Du, W. Chen, X.-L. Chen, and S.-L. Zhu, Exotic $QQ\bar{q}\bar{q}$, $QQ\bar{q}\bar{s}$, and $QQ\bar{s}\bar{s}$ states, *Phys. Rev. D* **87**, 014003 (2013), [arXiv:1209.5134 \[hep-ph\]](#).
- [77] W. Chen, T. G. Steele, and S.-L. Zhu, Exotic open-flavor $bc\bar{q}\bar{q}$, $bc\bar{s}\bar{s}$ and $qc\bar{q}\bar{b}$, $sc\bar{s}\bar{b}$ tetraquark states, *Phys. Rev. D* **89**, 054037 (2014), [arXiv:1310.8337 \[hep-ph\]](#).
- [78] Z.-G. Wang and Z.-H. Yan, Analysis of the scalar, axialvector, vector, tensor doubly charmed tetraquark states with QCD sum rules, *Eur. Phys. J. C* **78**, 19 (2018), [arXiv:1710.02810 \[hep-ph\]](#).
- [79] Z.-G. Wang, Analysis of the Axialvector Doubly Heavy Tetraquark States with QCD Sum Rules, *Acta Phys. Polon. B* **49**, 1781 (2018), [arXiv:1708.04545 \[hep-ph\]](#).
- [80] S. S. Agaev, K. Azizi, and H. Sundu, Double-heavy axial-vector tetraquark $T_{bc;\bar{u}\bar{d}}^0$, *Nucl. Phys. B* **951**, 114890 (2020), [arXiv:1905.07591 \[hep-ph\]](#).
- [81] S. S. Agaev, K. Azizi, and H. Sundu, Strong decays of double-charmed pseudoscalar and scalar $cc\bar{u}\bar{d}$ tetraquarks, *Phys. Rev. D* **99**, 114016 (2019), [arXiv:1903.11975 \[hep-ph\]](#).
- [82] L. Tang, B.-D. Wan, K. Maltman, and C.-F. Qiao, Doubly heavy tetraquarks in QCD sum rules, *Phys. Rev. D* **101**, 094032 (2020), [arXiv:1911.10951 \[hep-ph\]](#).
- [83] Q.-N. Wang and W. Chen, Fully open-flavor tetraquark states $bc\bar{q}\bar{s}$ and $sc\bar{q}\bar{b}$ with $J^P = 0^+, 1^+$, *Eur. Phys. J. C* **80**, 389 (2020), [arXiv:2002.04243 \[hep-ph\]](#).
- [84] M. Wagner (ETM), Static-Static-Light-Light Tetraquarks in Lattice QCD, *Acta Phys. Polon. Supp.* **4**, 747 (2011), [arXiv:1103.5147 \[hep-lat\]](#).
- [85] P. Bicudo and M. Wagner (European Twisted Mass Collaboration), Lattice QCD signal for a bottom-bottom tetraquark, *Phys. Rev. D* **87**, 114511 (2013), [arXiv:1209.6274 \[hep-ph\]](#).
- [86] Z. S. Brown and K. Orginos, Tetraquark bound states in the heavy-light heavy-light system, *Phys. Rev. D* **86**, 114506 (2012), [arXiv:1210.1953 \[hep-lat\]](#).
- [87] Y. Ikeda, B. Charron, S. Aoki, T. Doi, T. Hatsuda, T. Inoue, N. Ishii, K. Murano, H. Nemura, and K. Sasaki, Charmed tetraquarks T_{cc} and T_{cs} from dynamical lattice QCD simulations, *Phys. Lett. B* **729**, 85 (2014), [arXiv:1311.6214 \[hep-lat\]](#).
- [88] A. L. Guerrieri, M. Papinutto, A. Pilloni, A. D. Polosa, and N. Tantalo, Flavored tetraquark spectroscopy, *Proceedings, 32nd International Symposium on Lattice Field Theory (Lattice 2014): Brookhaven, NY, USA, June 23-28, 2014*, *PoS LATTICE2014*, 106 (2015), [arXiv:1411.2247 \[hep-lat\]](#).
- [89] P. Bicudo, K. Cichy, A. Peters, and M. Wagner, BB interactions with static bottom quarks from lattice QCD, *Phys. Rev. D* **93**, 034501 (2016), [arXiv:1510.03441 \[hep-lat\]](#).
- [90] P. Bicudo, K. Cichy, A. Peters, B. Wagenbach, and M. Wagner, Evidence for the existence of $ud\bar{b}\bar{b}$ and the nonexistence of $ss\bar{b}\bar{b}$ and $cc\bar{b}\bar{b}$ tetraquarks from lattice QCD, *Phys. Rev. D* **92**, 014507 (2015), [arXiv:1505.00613 \[hep-lat\]](#).
- [91] A. Peters, P. Bicudo, L. Leskovec, S. Meinel, and M. Wagner, Lattice QCD study of heavy-heavy-light-light tetraquark candidates, *Proceedings, 34th International Symposium on Lattice Field Theory (Lattice 2016): Southampton, UK, July 24-30, 2016*, *PoS LATTICE2016*, 104 (2016), [arXiv:1609.00181 \[hep-lat\]](#).
- [92] P. Bicudo, J. Scheunert, and M. Wagner, Including heavy spin effects in a lattice QCD study of static-static-light-light tetraquarks, *Proceedings, 34th International Symposium on Lattice Field Theory (Lattice 2016): Southampton, UK, July 24-30, 2016*, *PoS LATTICE2016*, 103 (2016), [arXiv:1609.00548 \[hep-lat\]](#).
- [93] P. Bicudo, J. Scheunert, and M. Wagner, Including heavy spin effects in the prediction of a $b\bar{b}ud$ tetraquark with lattice QCD potentials, *Phys. Rev. D* **95**, 034502 (2017), [arXiv:1612.02758 \[hep-lat\]](#).
- [94] A. Francis, R. J. Hudspith, R. Lewis, and K. Maltman, Lattice Prediction for Deeply Bound Doubly Heavy Tetraquarks, *Phys. Rev. Lett.* **118**, 142001 (2017), [arXiv:1607.05214 \[hep-lat\]](#).
- [95] A. Francis, R. J. Hudspith, R. Lewis, and K. Maltman, Heavy and light spectroscopy near the physical point, Part II: Tetraquarks, *Proceedings, 34th Inter-*

- national Symposium on Lattice Field Theory (Lattice 2016): Southampton, UK, July 24-30, 2016, PoS LATTICE2016*, 132 (2016).
- [96] P. Bicudo, M. Cardoso, A. Peters, M. Pflaumer, and M. Wagner, $ud\bar{b}\bar{b}$ tetraquark resonances with lattice QCD potentials and the Born-Oppenheimer approximation, *Phys. Rev.* **D96**, 054510 (2017), [arXiv:1704.02383 \[hep-lat\]](#).
- [97] G. K. C. Cheung, C. E. Thomas, J. J. Dudek, and R. G. Edwards (Hadron Spectrum), Tetraquark operators in lattice QCD and exotic flavour states in the charm sector, *JHEP* **11**, 033, [arXiv:1709.01417 \[hep-lat\]](#).
- [98] A. Francis, R. J. Hudspith, R. Lewis, and K. Maltman, Evidence for charm-bottom tetraquarks and the mass dependence of heavy-light tetraquark states from lattice QCD, *Phys. Rev.* **D99**, 054505 (2019), [arXiv:1810.10550 \[hep-lat\]](#).
- [99] P. Junnarkar, N. Mathur, and M. Padmanath, Study of doubly heavy tetraquarks in Lattice QCD, *Phys. Rev.* **D99**, 034507 (2019), [arXiv:1810.12285 \[hep-lat\]](#).
- [100] L. Leskovec, S. Meinel, M. Pflaumer, and M. Wagner, Lattice QCD investigation of a doubly-bottom $\bar{b}bud$ tetraquark with quantum numbers $I(J^P) = 0(1^+)$, *Phys. Rev.* **D100**, 014503 (2019), [arXiv:1904.04197 \[hep-lat\]](#).
- [101] R. J. Hudspith, B. Colquhoun, A. Francis, R. Lewis, and K. Maltman, Lattice investigation of exotic tetraquark channels, *Phys. Rev. D* **102**, 114506 (2020), [arXiv:2006.14294 \[hep-lat\]](#).
- [102] P. Mohanta and S. Basak, Construction of $bb\bar{u}\bar{d}$ tetraquark states on lattice with NRQCD bottom and HISQ up and down quarks, *Phys. Rev.* **D102**, 094516 (2020), [arXiv:2008.11146 \[hep-lat\]](#).
- [103] T. E. O. Ericson and G. Karl, Strength of pion exchange in hadronic molecules, *Phys. Lett. B* **309**, 426 (1993).
- [104] N. A. Törnqvist, From the deuteron to deusons, an analysis of deuteronlike meson-meson bound states, *Z. Phys. C* **61**, 525 (1994), [arXiv:hep-ph/9310247](#).
- [105] G.-J. Ding, J.-F. Liu, and M.-L. Yan, Dynamics of hadronic molecule in one-boson exchange approach and possible heavy flavor molecules, *Phys. Rev. D* **79**, 054005 (2009), [arXiv:0901.0426 \[hep-ph\]](#).
- [106] S. Ohkoda, Y. Yamaguchi, S. Yasui, K. Sudoh, and A. Hosaka, Exotic mesons with double charm and bottom flavor, *Phys. Rev. D* **86**, 034019 (2012), [arXiv:1202.0760 \[hep-ph\]](#).
- [107] Z.-M. Ding, H.-Y. Jiang, D. Song, and J. He, Hidden and doubly heavy molecular states from interactions $D_{(s)}^{(*)}\bar{D}_{(s)}^{(*)}/B_{(s)}^{(*)}\bar{B}_{(s)}^{(*)}$ and $D_{(s)}^{(*)}D_{(s)}^{(*)}/B_{(s)}^{(*)}B_{(s)}^{(*)}$, (2021), [arXiv:2107.00855 \[hep-ph\]](#).
- [108] A. V. Manohar and M. B. Wise, Exotic $QQ\bar{q}\bar{q}$ states in QCD, *Nucl. Phys.* **B399**, 17 (1993), [arXiv:hep-ph/9212236 \[hep-ph\]](#).
- [109] Z.-W. Liu, N. Li, and S.-L. Zhu, Chiral perturbation theory and the $B\bar{B}$ strong interaction, *Phys. Rev. D* **89**, 074015 (2014), [arXiv:1211.3578 \[hep-ph\]](#).
- [110] H. Xu, B. Wang, Z.-W. Liu, and X. Liu, DD^* potentials in chiral perturbation theory and possible molecular states, *Phys. Rev.* **D99**, 014027 (2019), [arXiv:1708.06918 \[hep-ph\]](#).
- [111] B. Wang, Z.-W. Liu, and X. Liu, $\bar{B}^{(*)}\bar{B}^{(*)}$ interactions in chiral effective field theory, *Phys. Rev.* **D99**, 036007 (2019), [arXiv:1812.04457 \[hep-ph\]](#).
- [112] A. Esposito, M. Papinutto, A. Pilloni, A. D. Polosa, and N. Tantalo, Doubly charmed tetraquarks in B_c and Ξ_{bc} decays, *Phys. Rev. D* **88**, 054029 (2013), [arXiv:1307.2873 \[hep-ph\]](#).
- [113] Q. Qin and F.-S. Yu, Discovery potentials of double-charm tetraquarks, (2020), [arXiv:2008.08026 \[hep-ph\]](#).
- [114] E. Eichten, K. Gottfried, T. Kinoshita, K. D. Lane, and T.-M. Yan, Charmonium: The Model, *Phys. Rev.* **D17**, 3090 (1978), [Erratum: *Phys. Rev.* D21, 313(E) (1980)].
- [115] N. Isgur and G. Karl, Hyperfine interactions in negative parity baryons, *Phys. Lett.* **72B**, 109 (1977).
- [116] S. Godfrey and N. Isgur, Mesons in a relativized quark model with chromodynamics, *Phys. Rev.* **D32**, 189 (1985).
- [117] S. Capstick and N. Isgur, Baryons in a relativized quark model with chromodynamics, *Proceedings, International Conference on Hadron Spectroscopy: College Park, Maryland, April 20-22, 1985*, *Phys. Rev.* **D34**, 2809 (1986), [AIP Conf. Proc. 132, 267 (1985)].
- [118] A. De Rújula, H. Georgi, and S. L. Glashow, Hadron masses in a gauge theory, *Phys. Rev.* **D12**, 147 (1975).
- [119] Y. B. Zeldovich and A. D. Sakharov, Quark structure and masses of strongly interacting particles, *Yad. Fiz.* **4**, 395 (1966), [*Sov. J. Nucl. Phys.* 4, 283 (1967)].
- [120] R. L. Jaffe, Multiquark Hadrons. I. The Phenomenology of $Q^2\bar{Q}^2$ Mesons, *Phys. Rev.* **D15**, 267 (1977).
- [121] R. L. Jaffe, Multiquark Hadrons. II. Methods, *Phys. Rev.* **D15**, 281 (1977).
- [122] F. Buccella, H. Høgaasen, J.-M. Richard, and P. Sorba, Chromomagnetism, flavour symmetry breaking and S -wave tetraquarks, *Eur. Phys. J.* **C49**, 743 (2007), [arXiv:hep-ph/0608001 \[hep-ph\]](#).
- [123] H. Høgaasen, E. Kou, J.-M. Richard, and P. Sorba, Isovector and hidden-beauty partners of the $X(3872)$, *Phys. Lett.* **B732**, 97 (2014), [arXiv:1309.2049 \[hep-ph\]](#).
- [124] M. Karliner and J. L. Rosner, Baryons with two heavy quarks: Masses, production, decays, and detection, *Phys. Rev.* **D90**, 094007 (2014), [arXiv:1408.5877 \[hep-ph\]](#).
- [125] X.-Z. Weng, X.-L. Chen, and W.-Z. Deng, Masses of doubly heavy-quark baryons in an extended chromomagnetic model, *Phys. Rev.* **D97**, 054008 (2018), [arXiv:1801.08644 \[hep-ph\]](#).
- [126] X.-Z. Weng, X.-L. Chen, W.-Z. Deng, and S.-L. Zhu, Hidden-charm pentaquarks and P_c states, *Phys. Rev.* **D100**, 016014 (2019), [arXiv:1904.09891 \[hep-ph\]](#).
- [127] X.-Z. Weng, X.-L. Chen, W.-Z. Deng, and S.-L. Zhu, Systematics of fully heavy tetraquarks, *Phys. Rev. D* **103**, 034001 (2021), [arXiv:2010.05163 \[hep-ph\]](#).
- [128] H.-M. Chan, M. Fukugita, T. H. Hansson, H. J. Hoffman, K. Konishi, H. Hogaasen, and S. T. Tsou, Colour chemistry — A study of metastable multiquark molecules, *Phys. Lett.* **76B**, 634 (1978).
- [129] M. Fukugita, K. Konishi, and T. H. Hansson, Pseudobaryons, *Phys. Lett.* **74B**, 261 (1978).
- [130] K.-T. Chao, The $c\bar{c}q\bar{q}$ states, *Nucl. Phys.* **B169**, 281 (1980).
- [131] K.-T. Chao, The $(cc) - (\bar{c}\bar{c})$ (Diquark-Antidiquark) States in e^+e^- Annihilation, *Z. Phys.* **C7**, 317 (1981).
- [132] X.-H. Liu, L. Ma, L.-P. Sun, X. Liu, and S.-L. Zhu, Resolving the puzzling decay patterns of charged Z_c and Z_b states, *Phys. Rev.* **D90**, 074020 (2014), [arXiv:1407.3684 \[hep-ph\]](#).

- [133] G.-J. Wang, X.-H. Liu, L. Ma, X. Liu, X.-L. Chen, W.-Z. Deng, and S.-L. Zhu, The strong decay patterns of Z_c and Z_b states in the relativized quark model, *Eur. Phys. J.* **C79**, 567 (2019), [arXiv:1811.10339 \[hep-ph\]](#).
- [134] L.-Y. Xiao, G.-J. Wang, and S.-L. Zhu, Hidden-charm strong decays of the Z_c states, *Phys. Rev.* **D101**, 054001 (2020), [arXiv:1912.12781 \[hep-ph\]](#).
- [135] G.-J. Wang, L. Meng, L.-Y. Xiao, M. Oka, and S.-L. Zhu, Mass spectrum and strong decays of tetraquark $\bar{c}sqq$ states, *Eur. Phys. J. C* **81**, 188 (2021), [arXiv:2010.09395 \[hep-ph\]](#).
- [136] J. P. Ader, B. Bonnier, and S. Sood, Do we need “mock” diquoniums to explain narrow widths into $b\bar{B}$ channels?, *Orsay Wkshp.1979:XIII*, *Phys. Lett.* **84B**, 488 (1979).
- [137] I. M. Barbour and J. P. Gilchrist, The $N\bar{N}$ and $\pi\pi$ Decay Modes of Baryonium, *Z. Phys.* **C7**, 225 (1981), [Erratum: *Z. Phys.*C8,282(1981)].
- [138] W. Roberts, B. Silvestre-Brac, and C. Gignoux, Baryon-antibaryon decays of four-quark states, *Phys. Rev.* **D41**, 182 (1990).
- [139] X. Liu, H.-W. Ke, X. Liu, and X.-Q. Li, Exploring open-charm decay mode $\Lambda_c\bar{\Lambda}_c$ of charmonium-like state $Y(4630)$, *Eur. Phys. J.* **C76**, 549 (2016), [arXiv:1601.00762 \[hep-ph\]](#).
- [140] D. Strottman, Multiquark Baryons and the MIT Bag Model, *Phys. Rev.* **D20**, 748 (1979).
- [141] C. Gao, *Group Theory and its Application in Particle Physics (in Chinese)* (Higher Education Press, 1992).
- [142] G.-J. Wang, L. Meng, and S.-L. Zhu, Spectrum of the fully-heavy tetraquark state $QQ\bar{Q}'\bar{Q}'$, *Phys. Rev.* **D100**, 096013 (2019), [arXiv:1907.05177 \[hep-ph\]](#).
- [143] C. Deng, H. Chen, and J. Ping, Towards the understanding of fully-heavy tetraquark states from various models, *Phys. Rev. D* **103**, 014001 (2021), [arXiv:2003.05154 \[hep-ph\]](#).
- [144] L. Zhao, W.-Z. Deng, and S.-L. Zhu, Hidden-charm tetraquarks and charged Z_c states, *Phys. Rev.* **D90**, 094031 (2014), [arXiv:1408.3924 \[hep-ph\]](#).